Universitetet i Stavanger
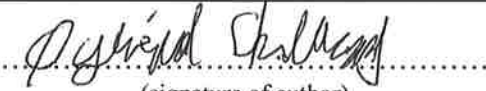
FACULTY OF SCIENCE AND TECHNOLOGY

MASTER'S THESIS

Study programme/specialisation: Automation And Signal Processing	Spring semester, 2018 Open
Author: Øyvind Wik Skadberg	*(signature)* (signature of author)
Programme coordinator: John Håkon Husøy Supervisor(s): Tomás Valbuena Montalvo	
Title of master's thesis: Radio Propagation & Technology In Offshore Communication Systems	
Credits: 30	
Keywords: Radio Propagation, fixed communication systems, mobile communication systems, LTE, offshore propagation	Number of pages: 109 + supplemental material/other: 6 Stavanger, 15.06.2018 date/year

Radio Propagation & Technology In Offshore Communication Systems

Øyvind Wik Skadberg

June 2018

MASTER THESIS

Faculty of Science and Technology

Department of Electrical Engineering and Computer Science

University of Stavanger

Abstract

This article is a Master thesis as part of the study program Automation and Signal Processing at the University of Stavanger, carried out during the spring of 2018. The thesis has been performed with close cooperation with Tampnet, a telecommunications company based in Stavanger, Norway, which specializes in high capacity, offshore communications. The idea for this thesis came out of the need for a single compilation of environmental factors affecting offshore communication systems. There was also a demand for an introductory piece on line-of-sight (LOS) radio links and Long-Term Evolution (LTE) technology for the employees of the network operations centre (NOC), which is what this thesis provides. This thesis consists of introductory elements to subjects such as wireless communication, environmental fading, interference, radio propagation, fixed communication systems and mobile communication systems. It also includes a section on some common difficulties related to the offshore environments such as tidal variations and multipath fading due to ocean reflections. These examples are supplemented with real-time data collected over years by the Tampnet NOC. The end result of the thesis as a whole is a ground-levelled preparatory collection to high-end courses within the field of radioelectric telecommunication.

Stavanger, 15.06.2018

———————————————

Øyvind Wik Skadberg

Acknowledgements

The first thank you goes to my supervisor this spring, Tomás. A huge thank you for always being there to answer my questions and for teaching me and introducing me to so many new subjects.

For continuous support throughout five long years, a warm gratitude goes to my partner and best friend, Anja. None of this would have been possible without you, which will never be forgotten.

Thank you John Håkon, for lecturing my first subject and more or less introducing me to to the field of communication, in addition to a friendly chat once a week during an eventful spring.

Ø.W.S.

Acronyms

3GPP The 3rd Generation Partnership Project

4G The forth generation of cellular network technologies

AC Alternating current

AWGN Additive white gaussian noise

BEC Backward error correction

BEC Bit error correction

BER Bit error rate

BLER Block error rate

BPSK Binary phase-shift keying

CCI Co-channel interference

CQI Channel quality indicator

DC Direct current

DFT Discrete Fourier transform

EMR Electromagnetic radiation

ENB/eNodeB Evolved Node B

FDD Frequency division duplex

FDMA Frequency division multiple access

FEC Forward error correction

FFT Fast Fourier transform

FM Frequency modulation

FSPL Free-space path loss

ICI Inter-carrier interference

IDU Indoor unit

IFFT Inverse fast Fourier transform

IF Intermediate frequency

ISI Intersymbol interference

ITU-R International Telecommunication Union - Radio communication

ITU International Telecommunication Union

K Kelvin

LDPC Low-density parity-check

LOS Line-of-sight

LTE Long-term evolution

MASL Metres above sea level

MCM Multi-carrier modulation

MIMO Multiple inputs multiple outputs

MME Mobility Management Entity

Mbps Megabits per second

NOC Network operations centre

ODU Outdoor unit

OFDMA Orthogonal frequency division multiple access

OFDM Orthogonal frequency division multiplexing

OSI Open systems interconnection

PAM Pulse amplitude modulation

QAM Quadrature amplitude modulation

QPSK Quadrature phase-shift keying

RB Resource blocks

RF Radio frequency

RLC Radio link control

RMS Root mean square

RSRP Reference signal received power

RSRQ Reference signal received quality

RSSI Received signal strength indicator

S-GW Serving gateway

SAE System Architecture Evolution

SC-FDMA Single carrier frequency division multiple access

SER Symbol error rate

SHF Super high frequency (3 GHz - 30 GHz)

SINR Signal-to-interference-plus-noise ratio

SISO Single input single output

SNR Signal-to-noise ratio

TDD Time division duplex

TDMA Time division multiple access

UE User equipment

UHF Ultra high frequency (300 MHz - 3 GHz)

Contents

List of Figures

List of Tables

Chapter 1

Introduction, Motivation & Background

1.1 Introduction

The purpose of this thesis is to provide an overview of the factors affecting radio wave propagation in offshore communication systems. The thesis provides basic explanations for all discussed subjects, meaning any reader with a basic knowledge of communication theory should be able to comprehend the contents.

This thesis has been written in cooperation with Tampnet AS, a telecommunications company based in Stavanger, Norway. The idea behind this thesis stems from the need for a compilation of ground-levelled radio wave propagation theory and examples, specifically for offshore environments. The object is for this compilation to be used by the network operation centre (NOC) to increase its competence within the subject of wireless communication.

The following list provides an overview of the chapters of this thesis, along with a short description of the topics contained in each chapter.

Radioelectric communication fundamentals
Laying out the fundamentals of wireless communication by electromagnetic waves. Topics include electromagnetic fields, antennas and noise.

Radio wave propagation

Descriptions on how the radio waves react as they travel through the air. Some topics include reflections, refraction, diffraction and why these effects cause losses in the electromagnetic field strength.

Terrestrial radio links

In this thesis, "radio links" refers to fixed communication systems, also called point-to-point systems. Terms like "LOS" and "microwave link" will also be used to refer to fixed systems. This chapter describes the functionality of such communication systems. Supplemented is a description of modulation and how noise affects the efficiency of communication links.

Mobile communication systems

Explanations on the infrastructure of mobile networks. Short introductions is also given to the network architecture and the functionality of the 4G technology, Long-term evolution (LTE).

Examples Of Offshore Propagation Impairments

Examples of offshore environmental occurrences, explaining how they affect the radio waves and how they can be identified from graphs of the received signal power.

1.2 Background

Ever since its introduction to telecommunication in the 1890s, electromagnetic waves and radio propagation has been studied intensively. For the first half of the 20th century, this resulted in some big accomplishments, such as widespread radio and TV broadcasting. While microwave links were researched as early as the 1930s, more focus was set on LOS and point-to-point transmission during and after World War II. Troposcattering is a communication technique developed in the 1950s and could, for its time, provide high-end, point-to-point communications for distances over 300 km. Troposcatter systems were used for, amongst other, oversea links, such as the "Pacific Scatter System", which connected Hawaii to Okinawa, on the coast of China. There is therefore a lot of material on radio propagation, for onshore, offshore and satellite

communications, but not a single collection of relevant material to the operations of Tampnet.

The NOC located in Norway oversee all the operations in Tampnet's North Sea network infrastructure. One of the responsibilities of the NOC is to troubleshoot LTE and fixed radio links. This thesis is therefore to act as a starting point for the NOC to increase its competence within the field of radio propagation, specifically factors resulting in signal degrading. In addition to boosting the general competence, a knowledge of radio propagation will help troubleshoot any incidents related to LTE and fixed radio links. The aim is for the NOC to be able to recognize and identify issues related to fading and interference, therefore resulting in a more prompt and thorough investigation.

1.3   Scope of the Thesis

The main focus of this thesis is radio propagation relevant to maritime environments. There are few prerequisites and the contents and explanations will stay on a parent level for most subjects, as the thesis is to act as preliminary material. Nonetheless, a background in engineering is recommended.

Introductions will be given to many aspects within the concepts of wireless communication. The main focus will be on the physical layer of the Open systems interconnection (OSI) model, however, there will be some information on the operations of radio links and LTE in the second layer.

In the chapter on radio propagation, equations will be presented on most subjects. This is so that the reader can see and understand the parameters of the total attenuation.

This thesis will focus on frequency bands below 25 GHz. Specifically, many of the graphs and examples will use the frequencies 800 MHz, 1800 MHz, 6 GHz and 12 GHz. This is because these are the mostly used bands for LTE and LOS within Tampnet's network.

Chapter 2

Radioelectric Communication Fundamentals

This chapter provides an introduction to some of the concepts regarding wireless communication that the reader should be familiar with. These include a beginner-level overview of the principles around radio waves, electromagnetic fields, antennas and noise.

2.1 Wireless Communication

From the perspective of this thesis, the concept of wireless communication means data transmission between two terminals using radio waves instead of an electrical conductor, e.g. a physical wire or cable. Communication in the form of sound waves nor the (visible) light spectrum will not be discussed in this thesis.

Advantages of wireless contra wired communication include accessibility, scalability and costs. However, the radio spectrum is a shared medium which heavily induces interference on the communication link between two ends. Another challenge of wireless communication is security, given the simplicity of an intruding receiver to listen to the signals transmitted between two ends. While security is an important issue of wireless communication, it will not be of focus in this thesis.

Radio waves propagate through the medium with a certain frequency. This frequency refers to the speed of the oscillations of the radiation's electric and magnetic

fields. By manipulation of the oscillations' amplitude, frequency or phase, one is able to transmit distinguishable symbols, recognizable at a receiving end, without the need of a wired connection between the two end points. This is the foundation of wireless communication.

2.2 Electromagnetic Fields

The following section digs into the principles and characteristics of radio waves. Radio waves are a subcategory of electromagnetic waves, or electromagnetic radiation (EMR). The electromagnetic spectrum have a number of uses, all depending on the waves' frequency. Radio waves are electromagnetic waves with a frequency between 3 kHz and 300 GHz. All telecommunication bands are situated within this spectrum.

An electromagnetic field consists of two parts: The electric field and the magnetic field. By *field*, we mean an area affected by a certain type of force. An electric field, for example, and is a space that is affected by an electric force. An electric force is the force which holds together electrons, while also being able to pull or push electrons, depending on the electric charge of the materials within the field. A magnetic field is created when electrons are moving. This ability to move electrons is what makes wireless communication possible. Figure 2.1 shows an illustration of an electromagnetic wave [1]. Here, the electric field is shown in blue, while the magnetic field is shown in red.
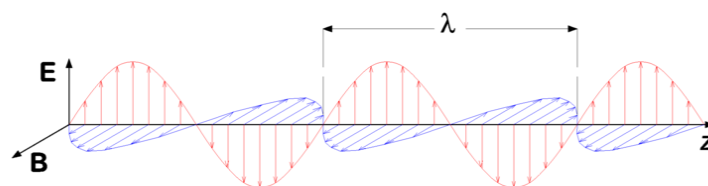
Figure 2.1: Illustration of an electromagnetic wave. The electric field is shown in red, where the axis marked "E" represents the field strength. The magnetic field is shown in blue, whrer the axis marked "B" is the magnetic field strength λ is the wavelength. The wave propagates towards the right. Image found from Wikimedia Commons, uploaded by user "P.wormer" [1].

EMR consists or a series of electric and magnetic forces with oscillating force strength, as shown in figure 2.1. The strength refers to the force's ability to move electrons. At the receiving end, these forces are used to push electrons inside the antenna, which is picked up by the receiver. This is explained in more detail in section 2.3.

The electric and magnetic fields are perpendicular relative to each other and are oscillating at the exact same frequency, while travelling at the speed of light. A single radio wave refers to one period of the oscillating electromagnetic field travelling away from the transmitter. The orientation of the field is called the "polarization" of the radio wave. The polarization depends on the orientation of the transmitting antenna itself. Some examples of polarization settings are vertical polarization and horizontal polarization. The names refer to the orientation of the electric field. In vertical polarization, the electric force is oscillating perpendicular to the Earth's surface. In horizontal polarization, the force oscillates parallel to the Earth's surface. The electric field is what moves the electrons within the receiving antenna, thus, the polarization has to be equal on both ends of the communication link.

2.3 Antennas

Because antennas are an essential part of a communication system, this section covers their most important functionalities, designs and purposes. This thesis will not cover the topic of antennas in detail, but rather give an overview how different types of communication systems require different types of antennas, based on the system requirements and objectives.

Antennas are, as commonly known, the objects used to transmit and receive electromagnetic waves. Antennas greatly vary in size and shape, depending on the type of communication system they are needed for. The shape and size of the antenna will naturally affect the shape of the induced electromagnetic fields. For example, an antenna intended for communication with outer space objects, would require a large, parabolic dish-shaped antenna so that the beam of transmitted radio waves become as narrow and concentrated as possible. Figure 2.2 show an example of parabolic, LOS antennas used for point-to-point radio links [2].

Figure 2.2: Photograph of parabolic dish antennas placed on an antenna tower [2].

Notice that in the case of LOS antennas, multiple antennas are pointed in the same direction. These are used for the same communication system, where the lower antenna is often used for what is called the "protection channel". When two or more channels are used for the same link, we achieve what is called *diversity*. This has a number of purposes, such as providing redundancy in case the main, upper antenna fails, or increasing the total bandwidth on the radio link, by both antennas transmitting separate data. Figure 2.3 shows an illustration of the antenna setup of a "space" diversity scheme, which is a diversity scheme where there are more than one antenna on one or both ends of the radio link.
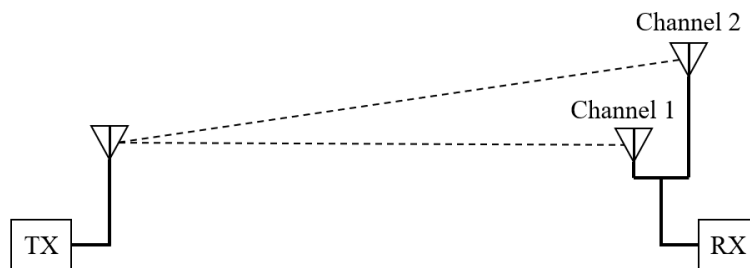
Figure 2.3: Illustration of space diversity, with two receiving antennas, and one transmitting antenna.

The communication system in the illustration consist of one transmit antenna and two receiver antennas. In the case of one of the channels going down, the communications link will stay up, as a result of having an active, backup channel. Diversity in general is discussed further in section 4.5.

In addition to parabolic antennas, there are also antennas intended for providing a spread coverage over a wide area, such as LTE or frequency modulation (FM) radio antennas. Figure 2.4 shows an example of LTE antennas in an LTE base station [3].

Figure 2.4: Photograph of LTE antennas placed on a tower, acting as a base station [3].

As with the LOS antennas, LTE antennas are also pointed in the same direction in pairs. This arrangement allows the antennas to provide the same coverage with two different carrier frequencies. The base station is then able to handle more units, while also providing redundancy.

2.3.1   Antenna Gain

The current generated by the receiving antenna is often incredibly small. Different types of antennas will naturally have variations in their capabilities of interpreting this current, and actually noticing it. This capability is measured as the *antenna gain* of the receiver. We also have the antenna gain of the transmitter, which describes its capability of converting the alternating current (AC) into proper radio waves. Take a cell phone for example. The receiver and transmitter on an ordinary phone are relatively small, while also being encapsulated by plastic or some other material penetrable by radio waves. Compare that to a parabolic dish, where the radio waves are bounced off the dish itself, and focused in on a single point. The receiving dish will naturally be able to sense the fields in a better fashion, and will therefore have a higher antenna gain factor.

Parabolic dishes, such as a satellite dish, are forms of something called high-gain antennas. High-gain antennas are recognizable by their parabolic shape, and is used for point-to-point communication, e.g. radio links. There are also low-gain antennas, which are used for point-to-area systems, e.g. LTE antennas as shown in figure 2.4. Both these types of antennas are still directional, meaning the fields are radiated in a certain direction. Another type of antenna are *omnidirectional antennas*, which radiate the field equally in all directions along one plane. Assuming no other losses, the field strength will therefore be equal in any direction, given the distance is the same. These types of antennas are useful for broadcasting purposes, such as FM radio, largely due to its simplicity.

The gain of an antenna is defined as the field intensity transmitted by the antenna, relative to the field intensity transmitted by an isotropic antenna. The field intensity is the amount of energy contained within a surface area unit of the transmitted wave. This gain, G_{dBi} can be measured by using equation 2.1.

$$G_{dBi} = 10log\frac{U}{U_{iso}}$$
(2.1)

where:

U is the transmitted radiation intensity,

U_{iso} is the isotropic radiation intensity.

The isotropic equivalent field is a hypothetical field transmitted by an isotropic antenna, where we assume no losses. An isotropic antenna is a theoretical model, in which the radio waves are transmitted in a perfect sphere fashion away from the transmitter, with equal radiated energy in every direction.

2.3.2   Functionality

Transmission antennas operate by supplying an oscillator with electrical direct current (DC), which in turn generates AC at a certain frequency. The AC is then modulated and amplified before reaching the radiating element. Modulation is explained in section 4.3. As the current flows through the radiating element, electromagnetic fields are created around it, oscillating at the same frequency as the AC, and travels away at the speed of light.[1] The fields radiate away from the element in a certain fashion, i.e. in a narrow, concentrated beam, or spread over a wider area, as explained in the previous section. This depends all on the shape of the antenna itself. The electromagnetic field travels at the speed of light, and provided the field strength does not get absorbed, a receiving antenna some distance away will be able to notice the oscillations.

Receiving antennas also have multiple structures and designs. Antennas used on cars, for example, is simply a metal wire, connected to the receiver itself. The electromagnetic forces originating from the transmitter, often a radio/telecommunications tower, generate a current in the metal wire, which is applied to an input on the receiver. In order for the receiver to interpret the current, it uses filters to separate out the desired frequency used by the transmitter. This is called tuning. In addition to the tuning filter, there are also several other types of signal processing tools one can use to recreate the current that flowed through the the radiating element at the receiver. Whichever tools and filters are used, the current is ultimately demodulated and converted back into a binary stream, in the case of a digital communication system. Ideally, this binary stream matches the one originating from the transmitter. The receiver's ability to recreate the data depends on several factors, one of which is the integrity of the radio waves after being transmitted through the air. The effects of the air and the transmission environment in general, is discussed in the following section, and following chapters.

---

[1]They do not actually propagate at the speed of light, as their actual speed depends on the transmission medium density. In this case, the medium is air, meaning the speed is just slightly lower.

2.4 Noise, Interference & Attenuation

This section describes the principles of the main forms of noise. Because noise is the main limiting factor in all forms of communication systems[2] and is the background for all propagation theory, it is a highly important subject to this thesis. For this section, the definition begins with an introduction to noise in general, then the subsections are divided into additive background noise and signal fading.

In terms of telecommunication, noise is unwanted effects and impairments to the transmitted signal. This means that the signal strength on the receiving end of a communication system will some amount of variation, depending on the amount of noise. Noise is the primary limiting factor in wireless communication, by limiting both receiver sensitivity and the overall bit rate.[3] Noise is the general term of disturbances caused to the radio waves, and effects such as interference and fading are what causes the noise. This section gives a description of some of the leading causes to signal noise, in addition to explanations of why they occur.

Some of the primary factors limiting the travelling distance are fading, the curvature of the Earth and blockage of the LOS. Transmission range also depends heavily on the carrier frequency of the signal. Fading effects due to the air itself, and its humidity, becomes more difficult to overcome as carrier frequency increases. This is one of the reasons why LTE operates at frequency bands around 800 or 1800 MHz. Another example is some WiFi routers used in regular homes that supports 5 GHz, in addition to the standard 2,4 GHz. In order to sufficiently use the 5 GHz band, the router cannot be placed in the first floor of a three story house, if any devices in the third floor requires the benefits of the potentially higher data rate a 5 GHz carrier provides.

---

[2]Noise is the limiting factor in both cabled and wireless systems.

[3]With a reduction in receiver sensitivity, the coverage is decreased. In other words, the reliable travelling distance of the radio waves decreases.

2.4.1   Background & White Noise

Background noise is electromagnetic fields which are picked up by the receiving end, but not transmitted by the appointed, transmitting end in the same system. Since it only adds to the net received power, it is called a form of *additive noise.* Background noise will be present in all communication systems and lays as a background to other, additional forms of noise, hence the name. Background noise is what we call "white noise". This means that its effect is equal to every frequency, i.e. it does not impact a certain frequency more than any other.

One usually model background noise as additive white gaussian noise (AWGN). AWGN is simply white noise that is added to the signal levels, where the noise "samples" has a Gaussian distribution in the time domain. The amount of background noise for a given channel can be found by muting the transmission on one end, and look at the received signal levels on the opposite end. One will always receive something on the other end. Background noise is caused by "thermal agitation" of the electrons which is formed in the conductor and other parts of the receiver. Thermal agitation is the random movement of electrons, caused by heat. It will therefore always be present, given the receiver is located in an environment above 0 kelvin (K).

2.4.2   Signal Fading

In vacuum, EMR would be able to propagate an unlimited distance. However, due to Earth's many obstructions, the transmission range is greatly reduced. Additionally, even though the waves themselves are able to travel some distance, "fading" will cause loss of the information in the radio waves. Fading is a subcategory of noise, as explained in the introduction of this section.

Fading is a wide term, and the general concept of instantaneous or temporary channel loss or unwanted change to the radio waves, causing variations in the received signal strength.[4] These losses are due to environmental effects and atmospheric conditions such as variations in temperature and air pressure, or moving obstructions in the transmission path. A simple example is when the waves travel along two or more sepa-

---

[4]While fading may also add or reduce signal power, it is not a "additive" form of noise, like background noise.

rate paths before arriving at the receiver. This results in what we call *multipath* fading. Each path is made by the signal reflecting or refracting off various objects, resulting in some loss of signal power and a slight phase shift due to the longer travelling distance.

Multipath fading is present in all radio links. However, their "damage" varies, as different technologies have different levels of resilience, and there are methods of reducing its' impact. One example used in LTE is orthogonal frequency division multiple access (OFDMA), which is more resilient towards multipath fading than previously used channel access methods such as narrowband time division multiple access (TDMA). In an offshore radio system, multipath fading occurs due to some waves reflecting off the ocean. Section 3.5 revisits this topic.

Chapter 3

Radio Wave Propagation

This chapter explains the principles behind radio wave propagation, i.e. how the waves react to the environment during transmission. It also includes an overview and explanation to some of the components of the total propagation loss. The sections expand upon the various components by providing detail and equations, most of which is taken from the International Telecommunication Union - Radio communication (ITU-R) recommendations. The object of this chapter is to visualize how much, and why, each component contribute to limiting the health of radio links and LTE connections.

3.1   Reflection & Refraction

This section gives an introduction to radio wave propagation theory, by explaining their general behaviour as they make contact with objects and environmental conditions. The aim is to set a foundation to the later sections in this chapter describing the attenuation components and parameters. As the title suggests, it covers the topic of reflection and refraction of radio waves when colliding with materials of another density than the main propagation medium.

Radio waves' collisions with various objects have different effects, depending on a number of factors. One effect already mentioned is scattering, where the wave is spread into multiple directions. Two other effects are "reflection" and "refraction". These occur due the change in the transmission medium density, e.g. travelling through the air and then the colliding object or material. In practice, this influences the waves'

phase velocity and splits up the wave's power, by some of the wave being bent towards to the denser material/medium, called *refraction*, and some bounce off the material, called *reflection*.

Reflection, refraction and absorption occurs at every surface collision the radio waves are exposed to, each hit resulting in a separation of the original radio wave power. Absorption occurs when the refracted waves are unable to penetrate the material, meaning their power is absorbed and most often transformed into heat. This is the principle of microwave ovens. Figure 3.1 shows a sketch of how radio waves react to a collision into a flat ocean surface. This figure, as with all other illustrations in this and following chapters, are own works produced by the author for the purpose of being presented in this thesis.
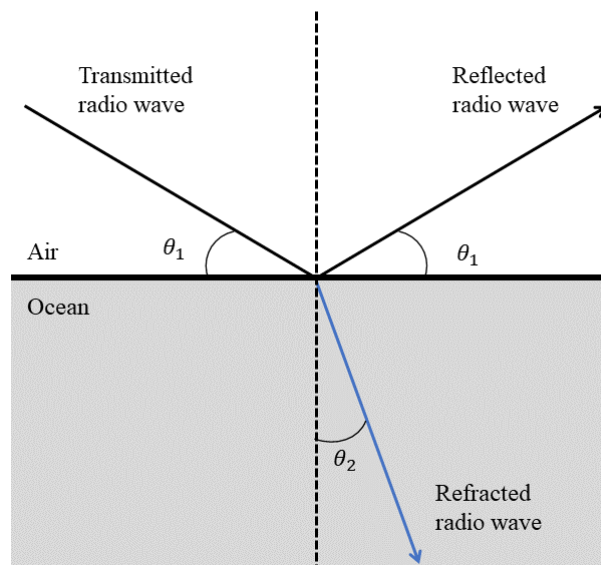
Figure 3.1: Geometry of radio wave reflection and refraction off an ocean surface with grazing angle θ_1.

The transmitted radio wave in this collision is often called the grazing ray, and the angle of reflection, θ_1, is called the grazing angle. Notice that the grazing angle is equal to the reflected radio wave's angle off the surface. The amount of the wave being refracted depends on the "refraction coefficient" of the surface. Seawater is generally highly reflective, meaning only a small part of the signal will be refracted and ultimately absorbed by the highly dense water. The reflectivity of seawater stems from its relatively high conductivity and dielectric constant. Having a high conductivity means

the material will block radio waves from getting absorbed or passing through, and reflect them instead. Steel is another example of a material of high conductivity, and is often a limiting factor in the wireless coverage inside a building or structure.

3.1.1 Dispersion

This section tries to illustrate the concept of dispersion of electromagnetic waves. While not directly relevant, it is a strong characteristic of the behaviour of radio waves, and therefore included in this thesis.

As waves are refracted, they are victims to a change in frequency. Dispersion is an effect that occurs when the phase velocity is determined by the wave frequency. The phase velocity is the speed a wave of a certain frequency component travel at.[1] As the waves are refracted and split into several frequencies, each component will be travelling at a different velocity. The different velocities means that each component will have a different refractive index. This can be shown by the definition of the refractive index, n, as shown in equation 3.1.

$$n = \frac{c}{v} \tag{3.1}$$

where:

c is the speed of light [m/s],

v is the phase velocity of light inside the material [m/s].

As shown by the equation, the refraction index decreases as the phase velocity increases. Generally after refraction, lower frequency waves will travel faster than high frequency waves. Dispersion can be witnessed by shining a light towards some glass at an angle, and see that a rainbow of colours will emerge on the other side. This same effect is illustrated in figure 3.2.

---

[1]In a signal built out of several carrier frequencies, a frequency *component* is the frequency of one of the carriers.
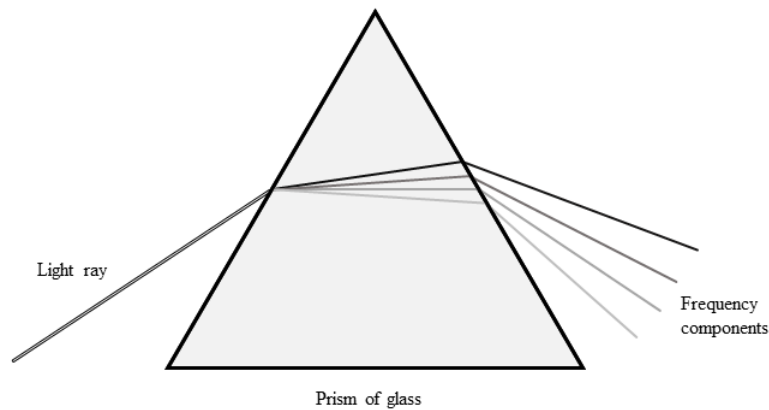
Figure 3.2: Illustration of dispersion of light through a prism of glass.

In the illustration, each shade of gray represents a unique frequency component. As seen in the figure, the frequency components of the white coloured light is split, due to each component having a different phase velocity, and therefore refractive index. The different refractive indexes causes a different degree of "bending" as the light passes through the glass.

The principle above also applies to microwave refraction. When waves collide with a surface of another density, the distribution of the amount of reflection and refraction depends on the type of material of the surface. The amount of dispersion therefore depends on the material. A "waveguide" for example, is extremely reflective.[2] This means that as the waves hit the walls inside the waveguide, they lose next to no power due to refraction, and more energy is conserved within the walls. The waves will therefore be less vulnerable to the effects of dispersion.

---

[2]A waveguide is a highly reflective "pipe" which guides the radio waves onto the ODU.

3.2   Atmospheric Refraction

This section describes how the atmosphere affects the direction of radio waves travelling through it. The description consists of an explanation of why this happens and its impact. The section is supplemented with figures on how the change in direction is dependent on the altitude.

As the radio waves travel through the atmosphere, they constantly collide with the molecules present in the air. The gradual change in the molecular density of the air causes the waves to bend towards the denser medium, as discussed in the previous section. This phenomenon is called *atmospheric refraction*, and holds the same principle as when colliding with objects. Because density in the atmosphere normally decreases with altitude, radio waves will bend towards the Earth surface. Figure 3.3 shows an exaggerated demonstration of how radio waves travel when transmitted from an antenna tilted upwards relative to the horizon.
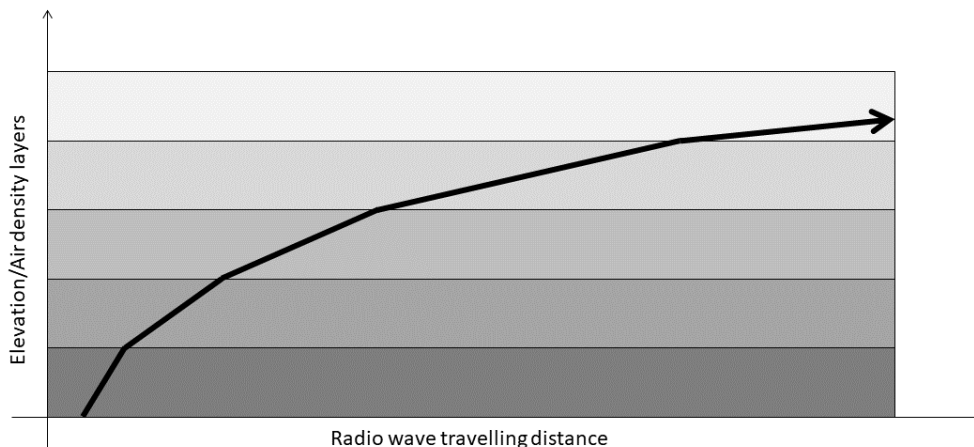
Figure 3.3: Conceptual illustration of atmospheric refraction of radio waves.

The y-axis represents different layers of air density, darker colours representing denser air, and vice versa. The arrow represents the propagation path of a radio wave getting refracted as it encounters a layer of different density. Assuming no other losses, i.e. the wave does not get absorbed in the air, it will continue to bend and eventually hit the Earth surface. The amount of radio wave bending is determined by the atmospheric refractive index.[3] This index is dependent on the temperature, air pressure and

---

[3]This index is the same as the refraction coefficient, but is a term used when specifically speaking of atmospheric refraction.

water vapour pressure in the air. According to Recommendation ITU-R P.453 [11], the equation for the atmospheric refractive index should be found using equation 3.2.

$$n = 1 + N \times 10^{-6}$$ (3.2)

where N is the radio refractivity, given by equation 3.3.

$$N = 77,6\frac{P}{T} + 72\frac{e}{T} + 3,75 \times 10^5 \frac{e}{T^2}$$ (3.3)

where:

P is the dry atmospheric pressure [hPa],

T is the air temperature [K],

e is the water vapour pressure [hPa].

Figure 3.4 shows how the atmospheric refractive index changes with altitude. The figure was made by implementing equation 3.1 into Matlab, as a function of height above the Earth's surface. The data used for this graph was taken from Recommendation ITU-R P.835 [12]. The data is only valid for locations above 45 °latitude, and is divided into averages of data collected through the yearly seasons of summer and winter.
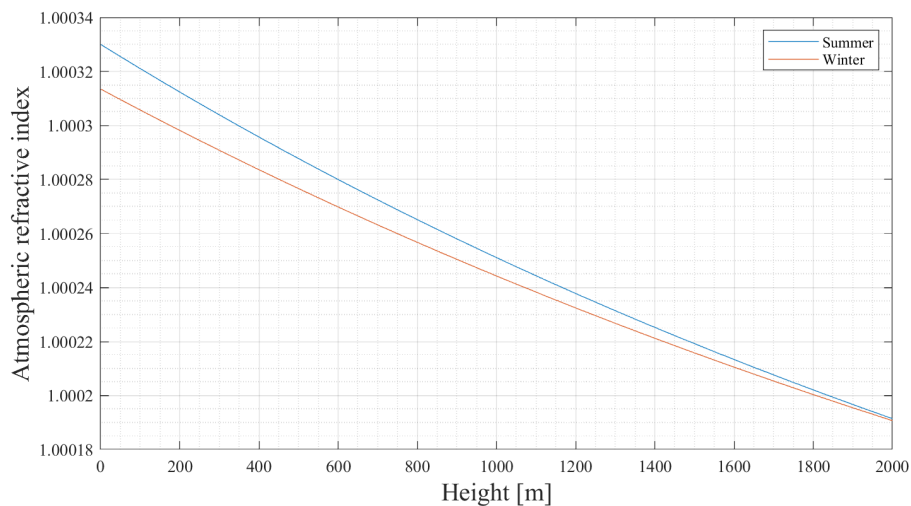
Figure 3.4: The atmospheric refractive index as a function of elevation above the Earth's surface.

From the graph, we see that the refractive index decreases with altitude. This makes sense, because normally the density of the atmosphere decreases with altitude, meaning that the radio waves will bend more the closer they are to the Earth's surface. Because the data from [12] is the average values across several months, it does not capture events of extreme conditions in is the atmospheric refraction. Three regularly occurring conditions in offshore environments are *sub-refraction*, *super-refraction* and *surface ducts*. These are explained in the following chapter.

3.2.1 Extreme Refractive Conditions

Extreme refractive conditions affect the radio wave propagation in different ways. During normal conditions, the waves will bend slightly towards the ground, which is explained in the previous section. This section discusses sub- and super-refraction, which causes abnormal radio wave bending.

Super-refractive conditions happen when a layer of extreme humid air lies directly on top of the ocean. If the air is humid enough, it will create what is called a surface duct, which is the even more extreme case of super-refraction. Because of the high density relative to the air above, the radio waves will be able to travel vast distances inside the duct, as they will continuously get refracted towards the ocean surface. Being trapped inside the duct enables the radio waves to reach areas beyond the visible horizon.[4]

Sub-refractive conditions, on the other hand, is a climatic state where the air density increases with elevation. Because radio waves bend towards the denser medium, they will turn away from the surface and travel upwards relative to the Earth's surface.[5] Figure 3.5 shows an illustration of the radio waves' behaviour during normal, super- and sub-refractive conditions.

---

[4]Inside a duct, radio waves can travel over 150 km. For reference, at 50 MASL one is able to see 25 km in any direction [13].

[5]Sub-refraction can be observed on very warm days, when distant "puddles" seems to appear along a road. This happens because the road warms air close to it, making it less dense than the air further above.
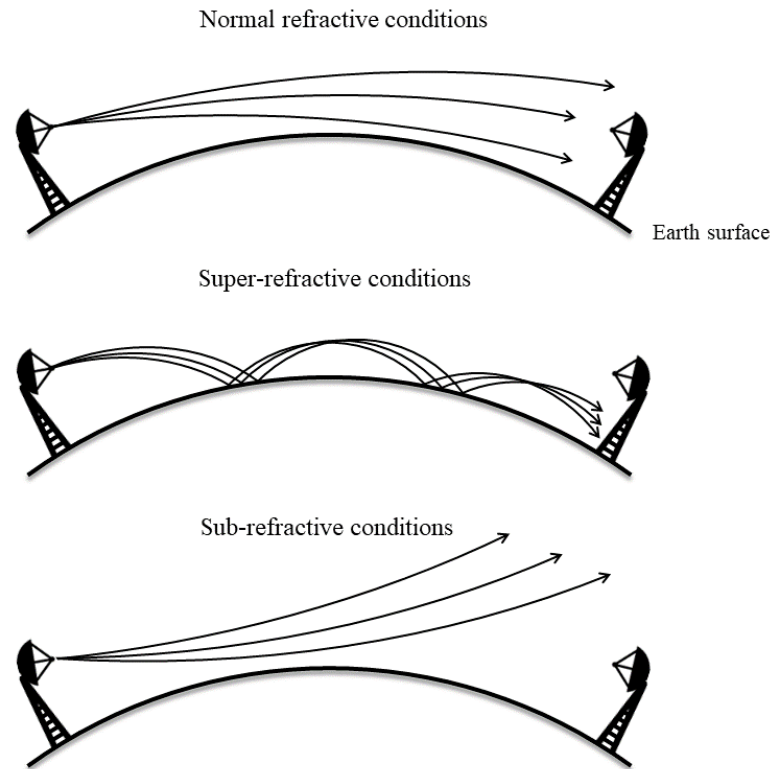
Figure 3.5: Conceptual illustration of radio waves' paths during normal, sub-refractive and super-refractive conditions [4] [5].

As seen in the figure, the upper communication system experiences normal refractive conditions, where the radio waves will bend somewhat towards the ground. As they bend with the curvature of the Earth, they will also be able to reach the receiver even though the two terminals cannot see each other. This is called *trans-horizon communication*. This can happen during super-refractive conditions, which might cause interference to other systems using a similar frequency band. The communication system in the lower part of the figure shows the effect of sub-refractive conditions.[6] In a worst case scenario, the link will become unusable, as little to none of the signals will even reach the receiver. Even when not considering the curvature of the Earth, sub-refraction is a big problem because the radio waves reaching the receiver are travelling very closely to the ocean surface. Therefore, during sub-refractive conditions, the communication link will be highly more vulnerable to obstructions, and crossing boats will be able to stop all communication in the system.

---

[6]These conditions heavily increase diffraction attenuation, which is explained further in section 3.8

3.3 Link Budget

For the purpose of providing an overview of is to be presented in the following sections, we firstly look at the link budget of a communications channel. The link budget is derived from the "Friis transmission formula", which was initially proposed by radio engineer Harald T. Friis. Friis wanted to express the received signal power based on the power density on the transmitted radio wave, antenna gains and distance, provided an ideal channel with no losses. The link budget, or the Friis transmission formula, is the general relationship between transmitted and received signal power, and is shown in equation 3.4.

$$P_r = P_t G_r G_t L \tag{3.4}$$

where:

> P_r is the received signal power [dBm],
>
> P_t is the transmitted signal power [dBm],
>
> G_t is the antenna gain of the receiver [dB],
>
> G_r is the antenna gain of the transmitter [dB],
>
> L is the various environmental losses [dB].

The rest of this chapter will cover the "environmental losses", L, part of the link budget. Signal power is commonly expressed using decibel units, as it is easier to perform calculations and they can provide a better overview of the performance of a communication system. Equation 3.5 shows the link budget in decibel units.

$$P_r = P_t + G_t + G_r - L \tag{3.5}$$

The antenna gain was briefly introduced in section 2.3.1, and is a central factor in determining the expected received power. This gain is a static variable for each antenna, specifying the antenna's efficiency, i.e. its capability of converting electrical current into radio waves, and vice versa. In addition to equation 2.1 in section 2.3.1, the antenna gain (G) can be found from equation 3.6.

$$G = \eta \left(\frac{\pi D}{\lambda} \right)^2 \tag{3.6}$$

where:

η is the antenna efficiency [%],

D is the reflector diameter [m],

λ is the signal wavelength [m].

The antenna gain will not be described any further during this thesis, as it is not directly connected to propagation losses. The gain will vary from one antenna to another, and is found on a case-by-case basis.

An offshore communication system is a typical two-ray model, in that addition to the direct LOS path, a large part of the total received field strength will be reflected by the sea surface before reaching the receiving antenna. Frequencies above 30 MHz penetrate or are absorbed by the ionosphere, making them negligible in the multipath model. Thus, from the perspective of this thesis, the received signal, $r(t)$, is represented as shown in equation 3.7.

$$r(t) = \alpha_1 s(t) + \alpha_2 s(t - \theta_1) \tag{3.7}$$

where:

r(t) is the received signal as a function of time,

s(t) is the transmitted signal as a function of time,

α_1 is the loss factor in the direct LOS path due to environmental attenuation,

α_2 is the loss factor in the reflected path via the ocean surface,

θ_1 is the time delay of the reflected signal via the ocean.

The objective of this chapter is to make the reader aware of some of the parameters that determine these loss factors and phase shifts. The following sections will describe some common parameters.

3.4 Free-Space Path Loss

The free-space path loss (FSPL) is the most basic of losses. The FSPL is not an attenuation factor like other environmental effects. The FSPL is defined as the received signal power in relation to a hypothetical, isotropic signal power. It is a loss due to the electromagnetic energy spreading over an expanding sphere, as the EMR propagate away from the transmitter. This loss is present in all radio communication, regardless of antenna polarization or direction. Figure 3.6 tries to illustrate FSPL by showing how two areas of equal field strength, a_1 and a_2, will have different densities at times T_1 and T_2.
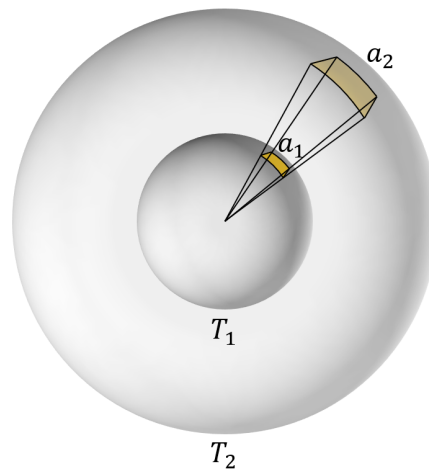
Figure 3.6: Illustration of the concept of FSPL. T_1 and T_2 are points in time, where T_1 < T_2. The spheres represent the isotropic radiation from the antenna in the centre. a_1 is the field strength in an arbitrary area, at time T_1. a_2 has the same field strength as a_2, but with a lower strength density.

As shown in the illustration, the observed power at a single point within area a_2 will be smaller than that in a_1. The FSPL can be expressed in either signal wavelength or frequency, as shown in equations 3.8 and 3.9, or in decibel units as in equation 3.10.

$$FSPL = \left(\frac{4\pi d}{\lambda}\right)^2 \tag{3.8}$$

$$FSPL = \left(\frac{4\pi d f}{c}\right)^2 \tag{3.9}$$

$$FSPL_{dB} = 20\log_{10}(d) + 20\log_{10}(f) + 32,44 \tag{3.10}$$

where:

d is the distance between transmitter and receiver [km],

λ is the signal wavelength [µm],

f is the signal frequency [MHz],

c is the speed of light (300000 km/s).

To visualize how much the FSPL contributes to the total attenuation, figure 3.7 shows a graphed version of equation 3.10. The graph was made by implementing equation 3.10 into Matlab. The graph shows the FSPL for commonly used frequencies within Tampnet's network between 800 MHz and 12 GHz for distances up to 60 km.
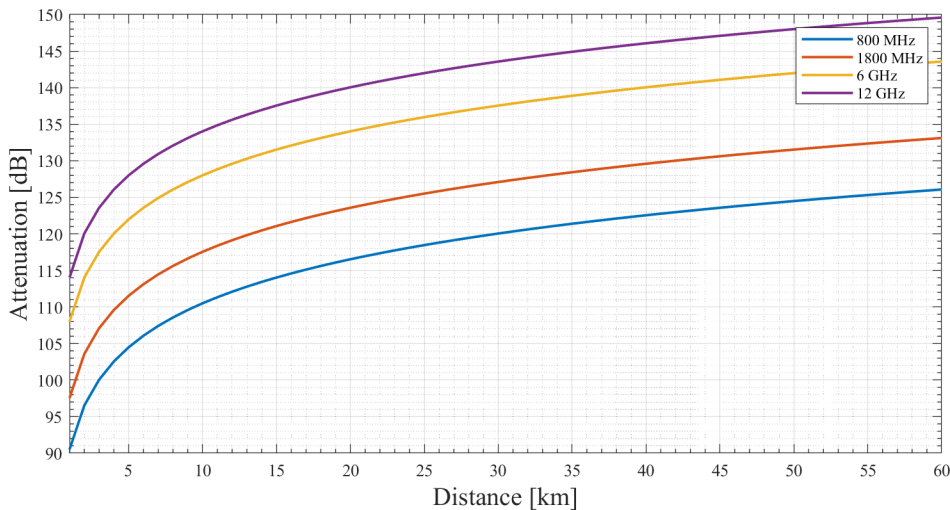
Figure 3.7: FSPL for distances up to 60 km, for frequencies 800 MHz, 1800 MHz, 6 GHz and 12 GHz.

As seen in figure 3.7 and equation 3.10, the attenuation increases with both frequency and distance. The FSPL is most often the highest attenuator in radio and LTE links. This is because it is the main factor in accounting for the propagation distance. Because of its significance, in some cases the FSPL may be seen as the sole factor for the propagation losses. Some examples include very short communication distances or in cases where the transmission medium is vacuum. In these cases, the FSPL can be used as a model for determining the expected received signal strength. These models are called "radio propagation models", and are used to provide accurate link budgets. The

FSPL propagation model can be created by inserting equation 3.8 into the link budget in equation 3.4. We then get the following:

$$P_r = P_t G_t \left(\frac{\lambda}{4\pi d}\right)^2 G_r \tag{3.11}$$

$$\frac{P_r}{P_t} = G_t \left(\frac{\lambda}{4\pi d}\right)^2 G_r \tag{3.12}$$

Equation 3.12 represents the ratio between the received and transmitter power, or a very simple propagation model, when only considering the free space loss.

3.5 Reflections Off An Ocean Surface

This section describes in detail the reflection of radio waves off an ocean surface. The ocean reflection is explained by using the geometry and mathematics of the reflected radio wave field strength, followed by a visualization of much the reflected signal affect the overall received signal strength. The section ends with two subsections describing some of the the factors which will cause variations in the amount of reflection.

The radio wave reflected off the ocean will be exposed to a power reduction and phase shift, as stated with equation 3.7. Power is lost in reflection because some of the wave will be refracted into the ocean, meaning the total power will be split. For an electromagnetic wave, the amount of reflection depends on multiple factors, such as the conductivity and permeability of the reflection material surface, the signal polarization and the incident angle.

The amount of power reflected and refracted can be symbolized by the *mean coefficient*, C_M. Consider a radio wave reflecting of a surface. By expanding upon equation 3.12, we can express the ratio between the received and transmitted power before and after the reflection impact, as shown in equations 3.13 and 3.14, respectively.

$$\frac{P_{R,o}}{P_t} = G_t \left(\frac{\lambda}{4\pi d}\right)^2 G_r \tag{3.13}$$

$$\frac{P_{R,i}}{P_t} = G_t \left(\frac{\lambda}{4\pi d}\right)^2 G_r C_{M,reflection} \tag{3.14}$$

where:

$P_{R,o}$ is the electric field strength directly before reflection impact,

$P_{R,i}$ is the electric field strength directly after reflection impact.

By inserting equation 3.13 into 3.14 and separating $C_{M,reflection}$, we can express the mean coefficient as in equation 3.15.

$$C_{M,reflection} = \frac{P_{R,i}}{P_{R,o}} = \left| \frac{E_i}{E_o} \right|^2 \tag{3.15}$$

Where E_i is the electric field strength of the receiver input and E_o is the electric field strength of the transmitter output, i.e. the electric field strengths after and before the reflection occurs, respectively.

Before continuing with the mean coefficient, examine figure 3.8. This is a theoretical model of two of the paths taken by the radio waves as they travel between the transmitter and the receiver.
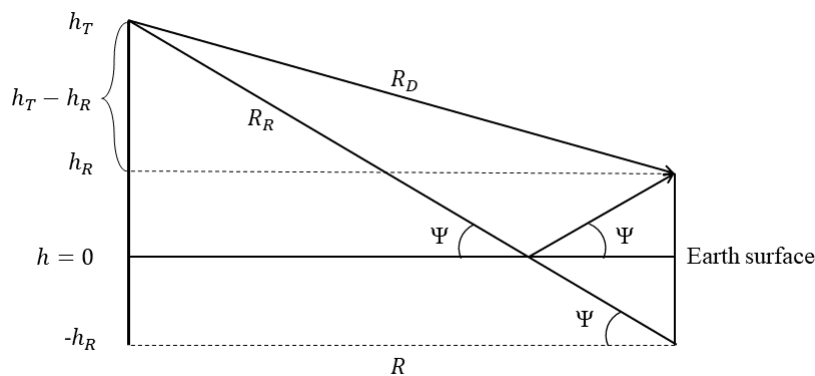
Figure 3.8: Geometry of a communication link with both a direct and a reflected path. h_T is the height of the transmitter, h_R is the height of the receiver, R_D is the length of the direct path, R_R is the distance between the transmitter and the point of reflection, Ψ is the grazing angle and R is the distance between the transmitter and the receiver, measured along the Earth's surface.

As seen in the figure, R is the distance between the antennas, R_D is the length of the direct, LOS path, R_R is the distance between the transmitter and the surface reflection point, h_T and h_R is the height of the transmitting and receiving antennas, respectively, and Ψ is the incident angle. Geometry tells us that R_D, R_R and Ψ can be represented

using the antenna heights, and the distance between them as parameters. Their relationship is shown in equation 3.16, 3.17 and 3.18.

$$R_D = \sqrt{(h_T - h_R)^2 + R^2} \tag{3.16}$$

$$R_R = \sqrt{(h_T + h_R)^2 + R^2} \tag{3.17}$$

$$\Psi = arctan\left(\frac{h_T + h_R}{R}\right) \tag{3.18}$$

Returning to the reflection coefficient and equation 3.15, we can express the electric field strengths in terms of the direct and reflected paths, using figure 3.8. The transmitted electric field strength will be equal to the direct path electric field strength and the received electric field strength will be equal to the sum of the direct and reflected electric field strengths. Thus, the mean coefficient can be rewritten as in equation 3.19.

$$C_{M,reflection} = \left|\frac{E_i}{E_o}\right|^2 = \left|\frac{E_D + E_R}{E_D}\right|^2 = \left|1 + \frac{E_R}{E_D}\right|^2 \tag{3.19}$$

where:

E_D is the electric field strength of the direct radio wave,

E_R is the electric field strength of the reflected radio wave.

These electric field strengths will have a relationship with the propagation distances and frequency equal to that of equations 3.20 and 3.21.

$$E_D \propto \frac{1}{R_D}e^{-jKR_D} \tag{3.20}$$

$$E_R \propto \frac{\rho}{R_R}e^{-jKR_R} \tag{3.21}$$

where:

$K = \frac{2\pi}{\lambda}$,

ρ is the reflection coefficient.

The reflection coefficient, ρ, is a factor dependent on the grazing angle, the conductivity and permittivity of the reflection surface, and the antenna polarization. Equations 3.22 and 3.23 shows the reflection coefficient for the vertical and horizontal polarization, respectively.

$$\rho_\perp = \frac{sin\Psi - \sqrt{\left(\epsilon_r - j\frac{\sigma}{2\pi f_c \epsilon_0}\right) - \cos^2\Psi}}{sin\Psi + \sqrt{\left(\epsilon_r - j\frac{\sigma}{2\pi f_c \epsilon_0}\right) - \cos^2\Psi}} \tag{3.22}$$

$$\rho_\parallel = \frac{\left(\epsilon_r - j\frac{\sigma}{2\pi f_c \epsilon_0}\right)sin\Psi - \sqrt{\left(\epsilon_r - j\frac{\sigma}{2\pi f_c \epsilon_0}\right) - \cos^2\Psi}}{\left(\epsilon_r - j\frac{\sigma}{2\pi f_c \epsilon_0}\right)sin\Psi + \sqrt{\left(\epsilon_r - j\frac{\sigma}{2\pi f_c \epsilon_0}\right) - \cos^2\Psi}} \tag{3.23}$$

where:

ϵ_r is the relative permittivity,

σ is the surface conductivity,

f_c is the signal carrier frequency,

ϵ_0 is the dielectric constant of vacuum.

Continuing equation 3.19, equations 3.24 - 3.26 shows the expansion of the ratio between the reflected and direct waves' electric field strengths, by inserting equations 3.20 and 3.21.

$$\frac{E_R}{E_D} = \frac{\frac{\rho}{R_R}e^{-jKR_R}}{\frac{1}{R_D}e^{-jKR_D}} \tag{3.24}$$

$$\frac{E_R}{E_D} = \frac{R_D}{R_R}\rho e^{-j(KR_R - KR_D)} = \frac{R_D}{R_R}\rho e^{-jK(R_R - R_D)} \tag{3.25}$$

$$\frac{E_R}{E_D} = \frac{R_D}{R_R}\rho e^{-jK\Delta R} \tag{3.26}$$

where:

$\Delta R = R_R - R_D.$

By neglecting all other losses, we are able to express the field strengths, E_D and E_R, using only the antenna gains.

$$E_D \propto \sqrt{G_T G_R} \tag{3.27}$$

$$E_R \propto \sqrt{G_T(\theta_i, \phi_i) G_R(\theta_r, \phi_r)} \tag{3.28}$$

$$\frac{E_R}{E_D} = \frac{\sqrt{G_T(\theta_i, \phi_i) G_R(\theta_r, \phi_r)}}{\sqrt{G_T G_R}} \tag{3.29}$$

Finally, the mean coefficient can be expressed as in equation 3.30.

$$C_{M,reflection} = \left| 1 + \frac{E_R}{E_D} \right|^2 = \left| 1 + \frac{R_D}{R_R} \rho \sqrt{\frac{G_T(\theta_i, \phi_r) G_R(\theta_r, \phi_r)}{G_T(\theta_i, \phi_i) G_R(\theta_i, \phi_i)}} e^{-jK\Delta R} \right|^2 \tag{3.30}$$

It it not trivial to look at equation 3.30 and understand how it effects the received signal strength. It is therefore necessary to simplify the expression. The following subsection describes an example of a valid simplification.

3.5.1   Grazing Angle Of 0°

For long distance radio links, an approximation of the mean coefficient can be made in order to simplify expression 3.30. This is done by assuming the grazing angle is 0°. This simplification is not too far off, and allows us to do what is shown in equations 3.31 - 3.34.

$$\Psi = arctan\left(\frac{h_T + h_R}{R}\right) \simeq 0 \tag{3.31}$$

$$\frac{R_D}{R_R} \simeq 1 \tag{3.32}$$

$$\rho_\perp \simeq \rho_\parallel \simeq -1 \tag{3.33}$$

$$G_T(\theta_i,\phi_i) \simeq G_T \atop G_R(\theta_r,\phi_r) \simeq G_R \Bigg\} \Rightarrow \sqrt{\frac{G_T(\theta_i,\phi_i)G_R(\theta_r,\phi_r)}{G_T G_R}} \simeq 1 \tag{3.34}$$

By inserting these into equation 3.30, we get the simplified function for the mean coefficient as shown in equation 3.35.

$$C_{M,reflection} = \left|1 - e^{-jK\Delta R}\right|^2 \tag{3.35}$$

where:

$K = \frac{2\pi}{\lambda}$,

$\Delta R = R_R - R_D$, i.e. the difference in path length between the reflected and direct path.

Thus, as the grazing angle approaches zero, the expression for the mean coefficient becomes significantly simpler. As mentioned, this simplification is not out-of-reach, as grazing angles are quite narrow to begin with, especially for long-distance LOS communication.

To visualize how the reflection affects the received signal strength, figure 3.9 shows the results of a Matlab experiment using equation 3.35. Here, the mean coefficient is given in dB units. The experiment shows the mean coefficient for frequencies 800 MHz, 1800 Mhz, 6 GHz and 12 GHz, and propagation distances between 10 and 50 km. For this experiment, the antenna heights for both ends was arbitrarily set to 50 meters above sea level (MASL). The figure is divided into two separate graphs. The upper graph fors the mean coefficient for distances between 10 and 50 km. The lower graph shows the mean coefficient for distances between 4 and 5 km.
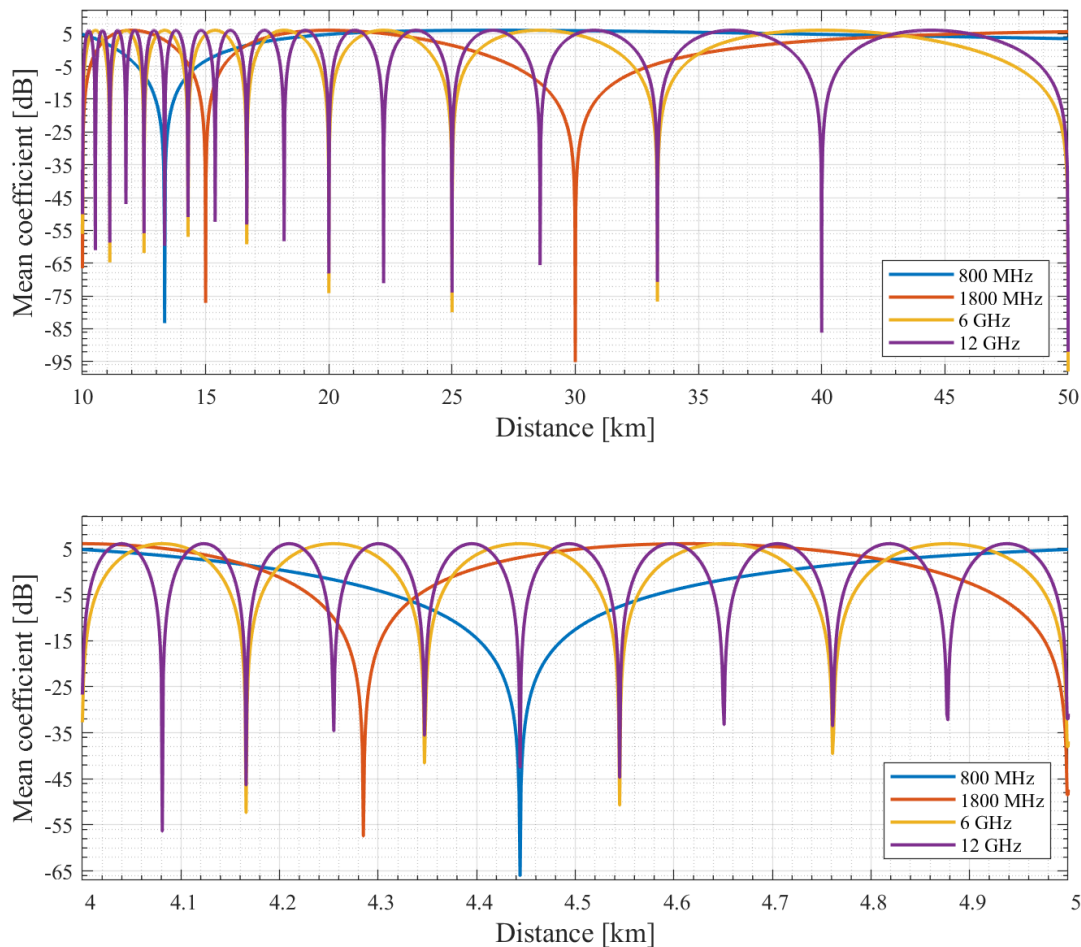
Figure 3.9: Mean coefficient for two-ray ocean surface reflection path. Frequencies 800 MHz, 1800 MHz, 6 GHz and 12 GHz. Propagation distances up to 50 km. Antenna heights of 50 m.

The spikes in the two graphs are the distances at which the field strength of the direct and reflected radio waves will cancel each other out, causing a massive drop in the overall, received strength. This is because of the phase difference caused by longer reflection path.[7] The interval between each spike increases with distance. This can be seen by comparing the upper and the lower graphs. The amount of spikes are also determined by the signal frequency[8] As the wavelength is shorter, the phase shift tolerance decreases. In other words, the phase of reflected wave does not need to be moved much before it will cancel the field strength of the waves on the direct path. This graph

---

[7]This must not be confused with ISI, which is interference caused by the amplitude of previous symbols. ISI is explained in section 4.4.

[8]For a clearer picture, one could say the spikes, or phase cancellations, depends on the wavelength, as this says more about the period of the field strengths. However, frequency is a favourable term, personally.

also displays that the LOS frequencies are much more victim to phase cancellation. Therefore, the frequency bands of short- to medium-distance LOS needs to be carefully planned in order to avoid cancellation by phase shift.

3.5.2 Divergence Factor

While figure 3.9 shows what one might expect out of the mean coefficient, it is valuable to know other affecting factors. This subsection, 3.5.2, and the next, 3.5.3, will try to explain two parameters which will cause variations in the reflections and thus, the mean coefficient.

As the distance between two terminals in a communication link increases, the curvature of the Earth will become more noticeable. The curved shape causes the reflected radio wave field to spread and scatter over a larger area, than what a completely flat surface would reflect. When the spreading increases, the radio wave field will cover a larger area, and less signal power will be received, as with the FSPL. Figure 3.10 contains an exaggerated visualization of how the curvature of the earth affects the reflection propagation path.
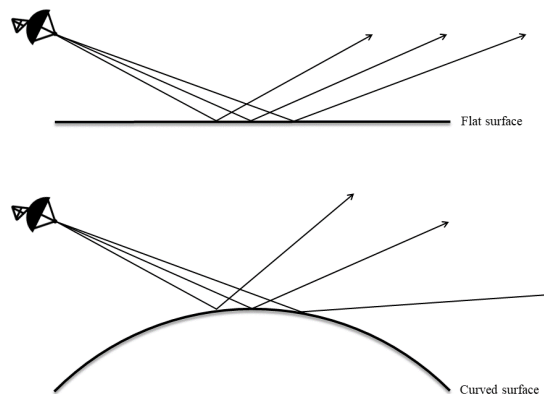
Figure 3.10: Conceptual illustration of radio wave reflecting off a flat surface and a curved surface [5].

As seen in the figure, the reflected field will be more spread because of the curvature. This curvature is accounted for in the form of the *divergence factor*. Equation 3.36 shows a widely accepted approximation of the divergence factor, D.

$$D = \left(1 + \frac{2}{a_e \sin\phi} \frac{l_1 l_2}{l_1 + l_2}\right)^{-\frac{1}{2}} \tag{3.36}$$

where:

a_e is the effective earth radius,

ϕ is the grazing angle,

l_1 is the distance from the transmitter to the point of reflection,

l_2 is the distance from the receiver to the point of reflection.

The relationship between the divergence factor and the reflection coefficient is shown in equation 3.37.

$$\rho = D\rho_0 \tag{3.37}$$

where:

ρ is the total reflection coefficient,

ρ_0 is the reflection coefficient given by equations 3.22 and 3.23.

By inserting this equation into equation 3.30, we have a mean coefficient which accounts for the Earth's curvature. From this, we can conclude that the graphs in figure 3.9 shows a worst-case scenario.

3.5.3 Rayleigh Criteria

Previous sections assumes the reflection surface is perfectly smooth, which in practice, it is not. The ocean surface is constantly changing and moving, which inflicts variations of the amount of reflections. The amount of variations in the height of the surface is called the *surface roughness*. In terms of the ocean, the roughness parameter is determined by the height of the ocean waves, naturally. However, the surface can often be approximated to be smooth, by following the Rayleigh criterion. The Rayleigh criterion states that if equation 3.38 below is satisfied, the surface can be seen as smooth.

$$d \geq \frac{\lambda}{8 sin \Psi} \tag{3.38}$$

where:

d is the root mean square (RMS) height of the ocean waves, measured from a reference plane at 0 MASL,

λ is the signal wavelength,

Ψ is the grazing angle.

Figure 3.11 shows the maximum allowed RMS height of the ocean waves for a surface to be classified as smooth, given the grazing angle and carrier frequency. The figure shows four examples of carrier frequencies: 800 MHz, 1800 MHz, 6 GHz and 12 GHz. Note that the RMS value is the squared average, meaning the ocean wave RMS height is more or less equal to the height or size of the waves, as their heights will all be similar.
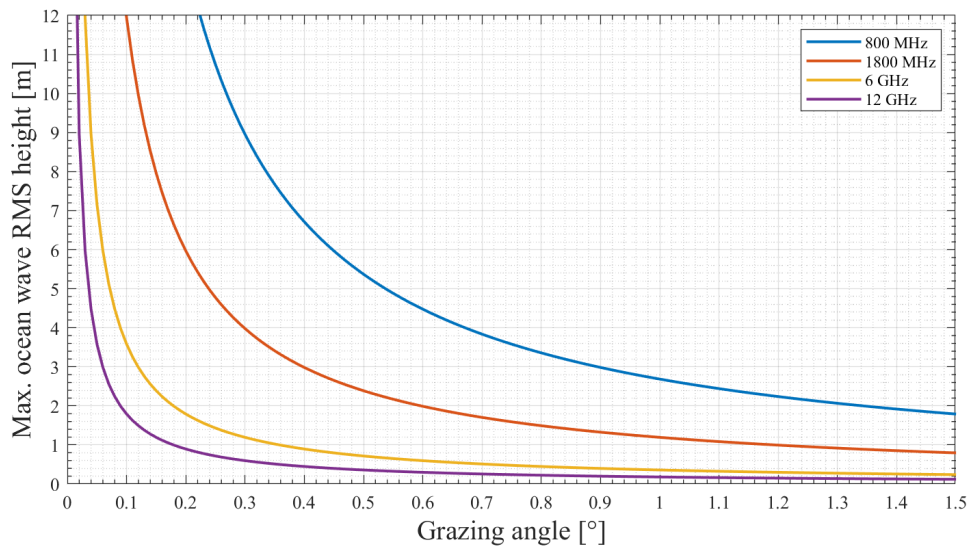
Figure 3.11: The maximum allowed height of ocean waves for the surface to be classified as smooth, given the grazing angle, according to the Rayleigh criteria. Graph shown for frequencies 800 MHz, 1800 MHz, 6 GHz and 12 GHz.

For a surface to be considered smooth, the characteristic parameters of the communication link should stay below the respective lines. For example, for a 12 GHz LOS, the waves should not surpass approximately 2 m in height if the surface is to be considered smooth, given a grazing angle of 0.1°. This ultimately means that radio waves with frequencies suitable for LTE, i.e. 800 and 1800 MHz, will still be reflective during periods of higher waves. The graphs in figure 3.9 will therefore more often fit LTE links, as these associated equations assume a smooth surface.

3.6   Attenuation Due To Hydrometeors

This section describes an attenuation factor caused by the environment, specifically hydrometeor attenuation. Hydrometeor is the common term for objects and particles in the atmosphere that is created by condensed water on the Earth. Some examples of hydrometeors are rain, snow and fog. The largest fading factor of hydrometeors in radio systems is most often the rain attenuation. This section includes the results of a Matlab experiment showing the amount of rain attenuation for different frequencies and rain rates. Following the example is a subsection on how rain can cause damage in the form of depolarization.

Rain attenuation is highly dependent on the carrier frequency, as stated earlier, and can therefore be neglected in a radio propagation model for LTE communication systems. However, radio links operating above 10 GHz may suffer greatly. Rain can be damaging because of its' scattering effect of the radio waves, which dampens the signal power and increases the multipath fading. Scattering of the signal means the radio wave hits an object and is reflected and refracted in several directions, each with a fraction of the original signal power. The amount of attenuation depends on the amount and size of the rain drops. In general, as the size of the wavelength gets closer to that of rain drop, the scattering and absorption becomes problematic. Similarly, snow is able to have the same attenuating effects as rain. Although, snow rate is significantly lower than rain, which makes it neglectable in radio links operating at frequencies below 20 GHz.

To display the degree at which rain affects the signal strength, figure 3.12 shows the attenuation in dB per km of rain the radio waves travel through. The formulas used to create the graphs, equations 3.39 through 3.41, is taken from Recommendation ITU-R P.838-3 [14]. The equations are only valid for vertical polarization.

$$\gamma_R = kR^\alpha \tag{3.39}$$

where:

γ_R is the rain attenuation per km for a given rain rate, R [dB/km],

k and α are coefficients determined by equations 3.40 and 3.41, respectively.

$$\log_{10} k = \sum_{j=1}^{4} a_j \exp\left[-\left(\frac{\log_{10} f - b_j}{c_j}\right)^2\right] + m_k \log_{10} f + c_k \tag{3.40}$$

$$\alpha = \sum_{j=1}^{5} a_j \exp\left[-\left(\frac{\log_{10} f - b_j}{c_j}\right)^2\right] + m_\alpha \log_{10} f + c_\alpha \tag{3.41}$$

where:

f is the signal frequency [GHz],

a_j, b_j, c_j, m_k, c_k, m_α and c_α are constants found from experimentation and given by TABLE 2 and TABLE 4 in [14].

Figure 3.12 shows the results of an example using equation 3.39. The figure is divided into four separate graphs, each representing a different rain rate. The rain rates are categorized into 4 different rain rates between 0.5 and 8 mm per hour. The attenuation is given in decibel per km for frequencies up to 24 GHz.
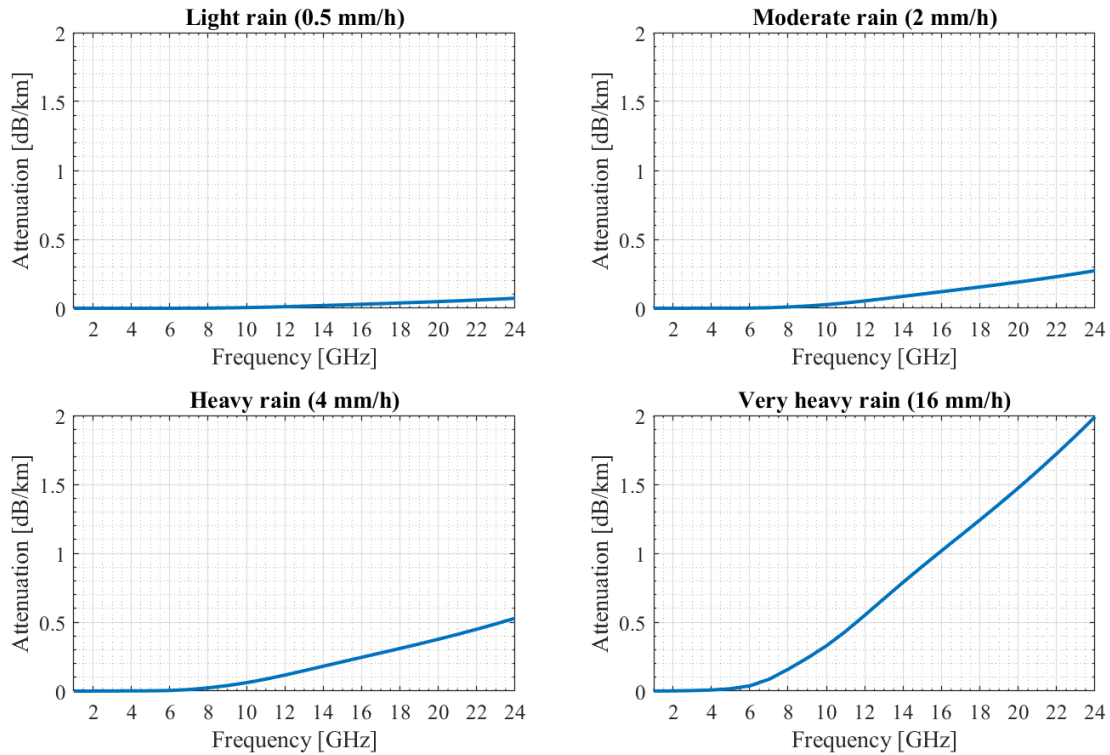
Figure 3.12: Rain attenuation in dB per km for four different rain rates, for frequencies up to 24 GHz.

From the figure, we can conclude that rain attenuation itself is more or less negligible as a whole for frequencies below 12 GHz. It will, however, be more noticeable for 24 GHz LOS links during periods of very heavy rain. For example, a 24 GHz link with distance of just 10 km will experience an additional 20 dB attenuation when the whole of the 10 km is affected by very heavy rain.

3.6.1 Depolarization

As seen in figure 3.12, the rain itself is not a direct cause of attenuation for frequencies below 12 GHz. However, hydrometeors also cause depolarization of the waves. As the name suggests, depolarization means that the orientation of the waves' amplitude oscillations are shifted. Depolarization is mainly an issue for satellite communication, due to the amount of free electrons within the ionosphere. Rain can, however, cause a similar effect, especially when the size of the rain drops increases.

Depolarization due to hydrometeors are not caused by the size of the rain drops themselves, but their shape. A perfectly symmetrical rain drop would not cause depolarization, but rather scatter the waves due to dispersion, ref. section 3.1.1. The problem arises when the rain drops become so large that their shape turn into ellipsoids. The problem escalates when wind is present, as this will slant the rain drops, causing more depolarization. This becomes more noticeable when the wind travels perpendicular to the radio link. The polarization of the waves are determined by the orientation of the transmitting antenna. At the receiving end, current is generated by the electrical field, as discussed in the previous chapter. In order for the waves to generate current, the oscillating amplitude of the electrical field must therefore line up with the orientation of the receiving antenna. If there is misalignment of the polarization and the antenna, the amplitude of the generated current will drop, and therefore lower the efficiency of the receiver. Depolarization can be a major issue if the communication system uses "polarization diversity". This is explained further in section 4.5.

3.7 Attenuation Due To Atmospheric Gases

The atmosphere consists of several layers. The lowest level, closest to the Earth's surface, is called the troposphere. The height of the troposphere is at its lowest over the poles, at approximately 7 km, and highest around the equator, at 17 km. Thus, in terrestrial microwave communication systems, all radio waves will be contained within this layer. This section shows how much the gases contained within the troposphere contribute to the total attenuation, by explaining how and why they damage radio waves. Then follows a summary of Recommendation ITU-R P.676 [15], and a Matlab experiment demonstrating the amount of loss atmospheric gases inflict.

The troposphere is the densest layer in the atmosphere, causing more disturbances than other layers to the radio waves. This disturbance caused by air in the troposphere is called *atmospheric gas attenuation*. The attenuation is a function of the air pressure, water vapour density, temperature, frequency and distance. The effect is caused by the oxygen and water vapour in the air, as the asymmetric polarization of water molecules cause them to attempt aligning with the electric field of the radio waves. This results in

radio wave refraction.

As described in section 3.2, the air causes constant collisions and disturbances to transmitted radio waves, in which they will bend towards the denser medium, through refraction. However, as we know, not all of the wave will be refracted, as some will be reflected and/or scattered. The power of the waves being reflected and/or scattered is so low, that they ultimately get absorbed by the air. This is what we call atmospheric gas attenuation or atmospheric gas absorption. The attenuation is caused by the oxygen molecules and the water vapour in the air, and the total gas attenuation is expressed by their sum.

Atmospheric gas attenuation is generally negligible for frequencies below 10 GHz, especially for short-range communications. However, it is included in this thesis for overview and clarification purposes. The total attenuation is largely dependent on the signal frequency, as there are several frequencies where the attenuation is greatly increased. These frequencies are determined by the resonances of the oxygen and water molecules. For example, one oxygen attenuation spike is for frequencies between 57 and 60 GHz, which is up to 15 dB per km. Meanwhile, around 10 GHz and 100 GHz, the oxygen attenuation is in the order of 0.01 dB per km. The principles surrounding this phenomena is not strictly relevant to this thesis and will not be discussed further. It is simply worth noting that some wavelengths are specifically vulnerable to either oxygen or water vapour attenuation.

Modelling the atmospheric gas attenuation is a large task, which can only be approximated. Recommendation ITU-R P.676-10 [15] provides a recommendation on an approximated model. The model described below is only applicable to frequencies below 54 GHz, and is still a heavy approximation. However, because the attenuation is generally low either way, the approximations are satisfactory. The model uses air pressure, temperature and water vapour density as parameters. These are used to find the oxygen and water vapour attenuation separately, before adding them and finding the total gas attenuation. The expression for oxygen and water vapour attenuation, γ_o and γ_w, which is used in ITU-R P.676-10 [15], is shown in equation 3.42 and 3.43, respectively.

$$\gamma_o = \left[\frac{7,2 r_t^{2,8}}{f^2 + 0,34 r_p^2 r_t^{1,6}} + \frac{0,62 \zeta_3}{(54-f)^{1,16\zeta_1} + 0,83\zeta_2} \right] f^2 r_p^2 \times 10^{-3} \qquad (3.42)$$

where:

$\zeta_1 = r_p^{0,0717} r_t^{-1,8132} e^{0,0156(1-r_p)-1,6515(1-r_t)}$,

$\zeta_2 = r_p^{0,5146} r_t^{-4,6368} e^{-0,1921(1-r_p)-5,7416(1-r_t)}$,

$\zeta_3 = r_p^{0,3414} r_t^{-6,5851} e^{0,2130(1-r_p)-8,5854(1-r_t)}$,

$r_t = \frac{288}{273+t}$,

$r_p = \frac{p_{tot}}{1013}$,

t is the temperature [°C],

p_{tot} is the total air pressure [hPa],

f is the signal frequency [GHz].

$$\begin{aligned}
\gamma_w = \{ &\frac{3,98\eta_1 e^{2,23(1-r_t)}}{(f-22,235)^2 + 9,42\eta_1^2} g(f,22) + \frac{11,96\eta_1 e^{0,7(1-r_t)}}{(f-183,31)^2 + 11,14\eta_1^2} \\
&+ \frac{0,081\eta_1 e^{6,44(1-r_t)}}{(f-321,226)^2 + 6,29\eta_1^2} + \frac{3,66\eta_1 e^{1,6(1-r_t)}}{(f-325,153)^2 + 9,22\eta_1^2} \\
&+ \frac{25,37\eta_1 e^{1,09(1-r_t)}}{(f-380)^2} + \frac{17,4\eta_1 e^{1,46(1-r_t)}}{(f-448)^2} \\
&+ \frac{844,6\eta_1 e^{0,17(1-r_t)}}{(f-557)^2} g(f,577) + \frac{290\eta_1 e^{0,41(1-r_t)}}{(f-752)^2} g(f,752) \\
&+ \frac{8,3328 \times 10^4 \eta_2 e^{0,99(1-r_t)}}{(f-1780)^2} g(f,1780) \} f^2 r_t^{2,5} \rho \times 10^{-4}
\end{aligned} \qquad (3.43)$$

where:

$\eta_1 = 0.955 r_p r_r^{0,68} + 0,006\rho$,

$\eta_2 = 0.735 r_p r_r^{0,5} + 0,0353 r_t^4 \rho$,

ρ is the water vapour density [$\frac{g}{m^3}$],

$g(f,f_i) = 1 + \left(\frac{f-f_i}{f+f_i} \right)$.

The total gas attenuation, A, is then given by equation 3.44.

$$A = \gamma r_0 = (\gamma_o + \gamma_w) r_0 \tag{3.44}$$

where:

γ is the sum of the oxygen and water vapour attenuation $[\frac{dB}{km}]$,

r_0 is the distance between the two terminals $[km]$.

Figure 3.13 shows the gas attenuation, A, in dB per km, for frequencies up to 25 GHz. The graph was made by implementing equation 3.44 into Matlab. In this experiment, air pressure was set to 1013 hPa, temperature to 5 °C and water vapour density to 7.5 $^g/_{m^3}$. These parameters were chosen to simulate a regular environment during winter months in the northern hemisphere.
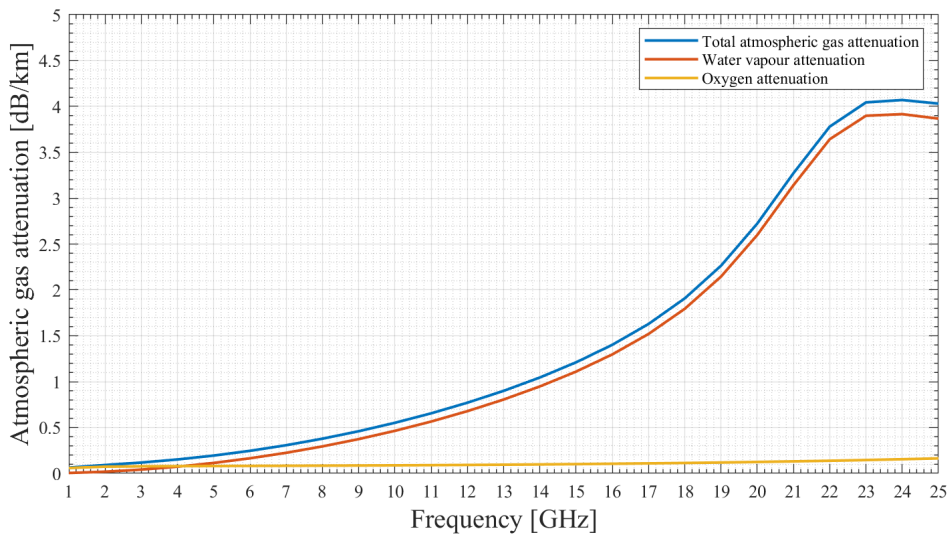
Figure 3.13: Atmospheric gas attenuation given in dB/km for carrier frequencies between 1 and 25 GHz.

As in the figure, oxygen attenuation is not the limiting factor for frequencies below 25 GHz. During normal conditions, attenuation caused by oxygen does not become an issue before reaching frequencies around 50 GHz. Moreover, LTE communication links can generally neglect gas attenuation as a whole, as the total attenuation the is close to 0 dB/km.

On the other side we have the water vapour attenuation, which accounts for most of the atmospheric absorption. The example above also assumed winter months, when the water vapour density is at its lowest. During the summer, it is possible for the the water vapour density levels to rise to 20 ^{g}/m³. To compare different water vapour density levels, figure 3.14 shows a graph of the total atmospheric gas attenuation in dB/km for water vapour densities between 5 and 20 ^{g}/m³. The graph shows the attenuation for frequencies 800 MHz, 1800 MHz, 6 GHz and 12 GHz.
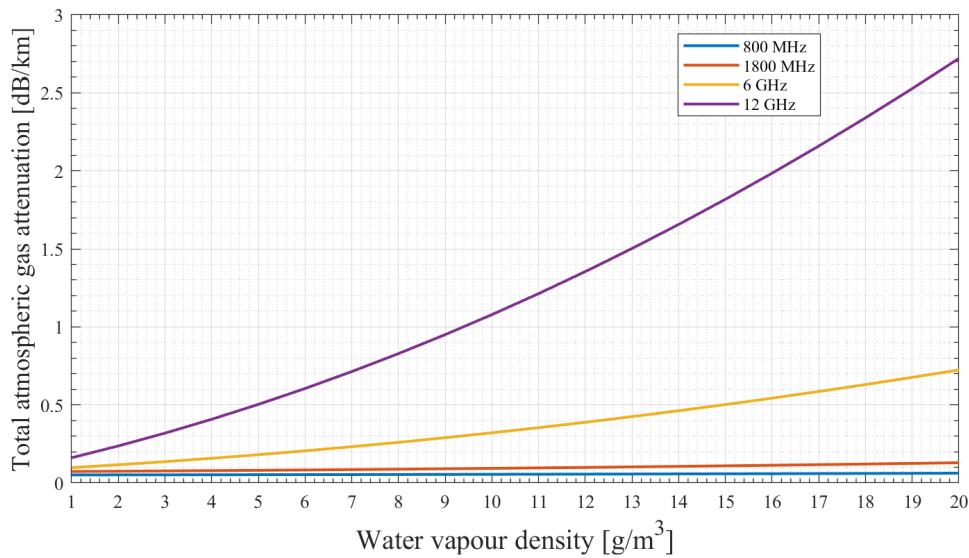
Figure 3.14: Atmospheric gas attenuation for frequencies 800 MHz, 1800 MHz, 6 GHz and 12 GHz for water vapour densities between 5 and 20 ^{g}/m³.

As seen in the figure, LTE bands do not suffer greatly from higher water vapour densities either. A 6 GHz radio wave would suffer to some degree, but only when travelling over long distances. 12 GHz radio waves will be greatly damaged, even for short- to mid-range distances. From this, we can see one of the reasons why bands above 10 GHz are not viable for long-distance offshore communication systems.

3.8   Diffraction Attenuation

Similar to reflection and refraction, *diffraction* is an effect that happens when a radio wave collides with an object. Diffraction is what we call the behaviour where some of the wave will bend around the colliding object. In radio communication, this means some signal power will be lost in the waves bending around the objects, and ultimately not reaching the receiver. Diffraction enables the radio waves to reach the shadow zone of obstructing objects.

Diffraction attenuation is associated with the disturbance of the LOS, meaning that as the propagation path gets more cluttered with various objects, the diffraction loss increases. Diffraction loss may be present regardless of a non-obstructed LOS between the transmitter and receiver. This is because we look at the transmission path as a field, or a "zone". Any obstacle in this field will act as a disturbance of the LOS. When determining if any objects are disturbing the LOS path, one usually looks at the "Fresnel Zone" [16]. Fresnel zones are ellipsoidal zones around the transmitter and receiver, and in order for diffraction attenuation to not be present in the system, these zones must be clear of obstacles. One is usually most interested in the first Fresnel zone, which is the narrowest and innermost field. Figure 3.15 shows an illustration of the first Fresnel Zone structure.
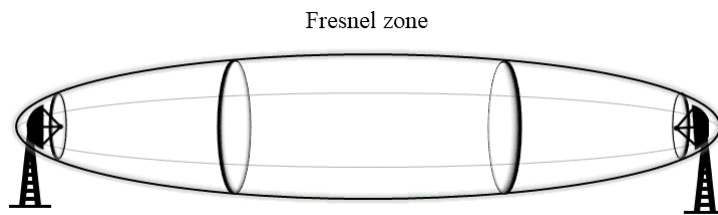
Figure 3.15: Illustration of the first Fresnel zone between two terminals [4] [5].

Every part of this zone is carrying field strength which is used at the receiving side of the communication link. As objects move into the zone, some of the wave gets refracted and ultimately power is lost. For the first Fresnel zone, diffraction attenuation does not cause an impact until the obstruction reaches 60% of the Fresnel zone radius. Figure 3.16 shows how much transmission power is lost due to diffraction, taken from Recommendation ITU-R P.530-17 [6]. The x-axis represents the clearance between an

object and the direct LOS path, and the y-axis shows the diffraction loss.

Diffraction loss for obstructed line-of-sight microwave radio paths

B: theoretical knife-edge loss curve
D: theoretical smooth spherical Earth loss curve, at 6.5 GHz and $k_e = 4/3$
A_d: empirical diffraction loss based on equation (2) for intermediate terrain
h: amount by which the radio path clears the Earth's surface
F_1: radius of the first Fresnel zone
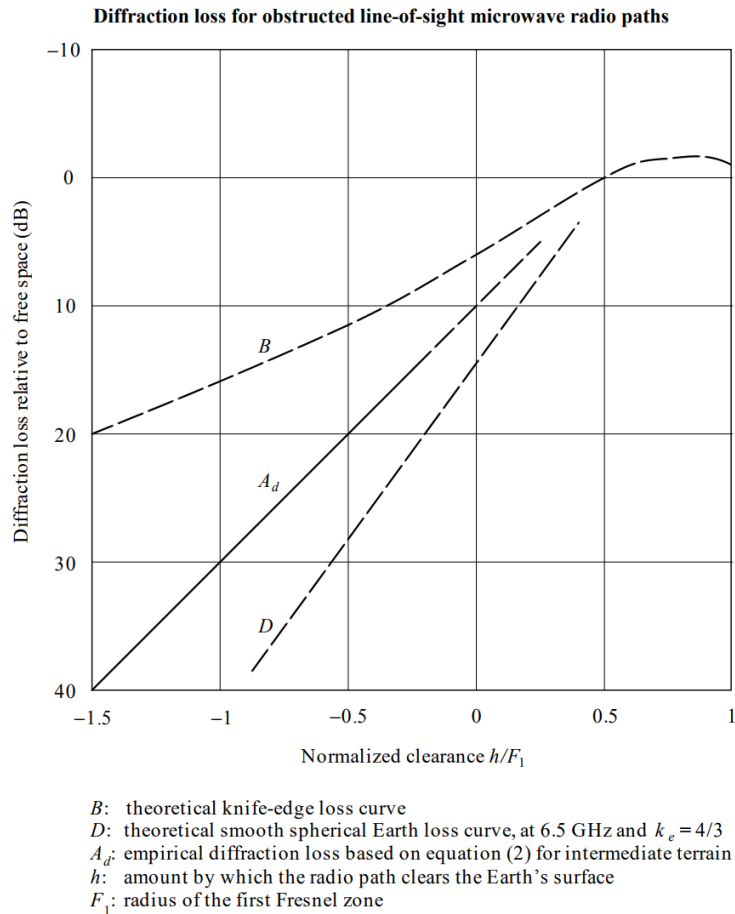
Figure 3.16: Diffraction loss for obstructed LOS microwave radio paths, from ITU-R P.530-17 [6].

As seen in the figure, the amount of attenuation depends on the shape of the obstructing object. The Earth gives the highest amount of diffraction loss, while a "knife-edge" object results in the lowest amount of loss. By knife-edge, one means the obstructing object is as thin as a knife's edge. Also note that between 0,5 and 1 normalized clearance, i.e. the object is outside the Fresnel zone, the diffraction loss is negative, meaning the object placement causes an increase in received signal power. This is a result of some of the radio waves reaching the receiver by reflecting off the object, thus adding another viable path, resulting in multipath fading.

For offshore communication systems, the tides can be seen as an object slowly moving into, and away from, the Fresnel zone. The effect of the tides is noticeable in long-range LOS communication, as the ocean surface will obstruct a large portion of the first Fresnel zone. This is shown further in section 6.2. During sub-refractive conditions, the rise in sea level alone can cause an outage in the communication link. Diffraction attenuation will always be present, however most noticeable during two main occasions. One of them is when a boat is travelling across the LOS. An example of this is shown in section 6.1. The other occasion is during sub-refractive tropospheric conditions, as discussed in 3.2.1.

3.9 Propagation Prediction Methods

The previous sections have described the expected attenuation for various effects that damages the field strength of the transmitted EMR. By combining each expected effect, one can create a prediction model for how much total attenuation loss one expects for a given communication link. These predictions are called propagation models.

Propagation models have the purpose of providing accurate link budgets. By having accurate link budget, one is able to carefully plan the carrier frequency, modulation scheme, coding technique, and so on, based on the total losses given by the propagation model [17]. As transmission power and antenna gains are known, one is able to use equation 3.5 to how much loss the link is able to endure.

3.9.1 Two-Ray Ground Reflection Model

The following section describes an example of a propagation model. The "two-ray ground reflection model" is based on the presumption that the transmitted signal travels only along two paths towards the receiver. The formula for the received power is shown in equations 3.45 and 3.46.

$$P_r(d) = \frac{P_t G_t G_r h_t^2 h_r^2}{d^4} \tag{3.45}$$

$$PL = P_{t_{dBm}} - P_{r_{dBm}} = 40\log_{10}(d) - 10\log_{10}(G_t G_r h_t^2 h_r^2) \tag{3.46}$$

where:

P_t is the transmitted signal power,

G_t is the transmitting antenna gain [dB],

G_r is the receiving antenna gain [dB],

h_t is the height of the transmitting antenna (MASL) [m],

h_r is the height of the receiving antenna (MASL) [m].

As seen from the equations, frequency is not a factor in this model. The model is derived from only the geometry of the communication system, i.e. the height of the antennas relative to the ground, the grazing angle and the reflection coefficient, amongst others. Figure 3.17 shows the predicted attenuation for distances up to 60 km, using equation 3.46.
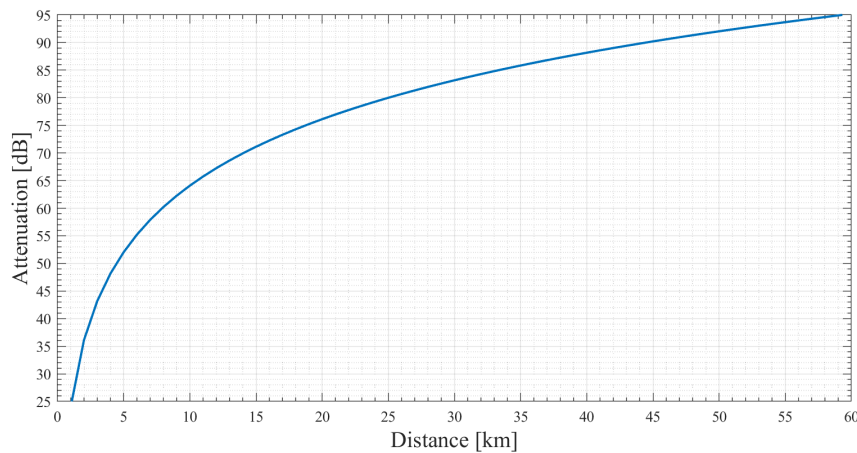
Figure 3.17: Predicted attenuation using the two-ray ground reflection model, for distances up to 60 km.

The two-ray model does not take any other attenuations into account. It is simply an alternative to using using the FSPL model. For long range radio links, the two-ray ground reflection model will often be more accurate than simply using the FSPL for prediction. For short propagation distances, however, i.e. less than 50 m, the FSPL is often sufficient. In order to make a more accurate prediction, one would have to consider various other attenuation components, such as atmospheric gas absorption and

diffraction. The International Telecommunications Union (ITU) has published a series of models, appropriate for various environments and scenarios. These are generally more popular due to higher prediction accuracy.

Chapter 4

Terrestrial Radio Links

This chapter covers the topic of terrestrial radio links, or microwave LOS. The Tampnet NOC ensure operation on a number of radio links located in the North Sea. The object of this chapter is to give the reader an insight into how radio links work in the physical layer, so that one better understands how and why errors occur. In understanding this, one can see how it correlates to the throughput and the operation in general.

4.1 Radio LOS Background

A radio link is a fixed, static, wireless connection between two end points. Large parabolic antennas, high elevation, direct LOS and fixed locations enable radio links to make use of higher carrier frequencies and larger frequency bands, with the help of link budgeting.

Radio links mostly make use of the super high frequency (SHF) radio band, meaning the radio waves are classified as *microwaves*, given their short wavelength (10 cm - 1 mm). Higher frequency bands correlates to higher bandwidth, meaning radio links are generally able to support high capacity traffic demands. This makes them a highly viable option when designing a static, wireless connection in a network infrastructure.

In radio links, there are two statically located terminals in each system: A transmitting antenna, and a receiving antenna. Both are often located on structures such as radio towers, or on oil platforms in the case of offshore systems. Because radio links are used as a "backbone" in a network infrastructure, they often have high demands in

terms of total data capacity. Thus, they require high bandwidth and therefore narrow wavelengths, or microwaves. As the frequency of the radio waves increase, they will be less prone to atmospheric refraction, and to some degree, rather travel in straight lines. In offshore systems, the main obstructing obstacle is the Earth's curvature, as mentioned in previous chapters, and the achievable length of the radio link is limited by the height of the antenna placements. In order for the antennas to see each other, they are therefore often placed on tall structures. Radio links with the end antennas in each other's line-of-sight are called LOS links.

LOS links are, as mentioned, used for backbone purposes. Thus, they can be seen as an alternative to fibre optic cables. The largest advantage of using LOS is low cost, especially offshore. This applies to both installation and operation of the link. Fibre optic cables offshore are incredibly expensive to install, and in the event of a fibre break, difficult to repair. However, as explained in earlier chapters, microwaves are disturbed by interference, fading and other noise.

4.2   Structure Of A Fixed LOS System

This section covers how a fixed radio link is structured, in terms of equipment and different main steps during transmission. Here, the following parts of a fixed radio system will be discussed: The modulator, the antennas, the receiver filter and the demodulator.

The modulator's purpose is to combine the data from an input source with the electrical AC from the oscillator. This means that it transforms the strictly sinusoid current from the oscillator, and outputs a stream of current which represents data, or binary values, it has been given by a data input source, such as a computer. The modulation is done by an "indoor unit" (IDU). Other tasks of the IDU include transform the radio frequency (RF) signal into an intermediate frequency (IF) signal, in addition to any signal processing. From the IDU, the modulated current, now at the IF, is transported to an "outdoor unit" (ODU). The ODU is either directly mounted onto the back of the antenna, or connected to the antenna through a waveguide. Tasks performed by the ODU include amplification and filtering, before converting the IF signal back

into an RF signal. From the ODU, the RF signal is sent through the radiating element of the antenna, which generate the radio waves. Figure 4.1 shows the transmission and receiving process in a communication system.
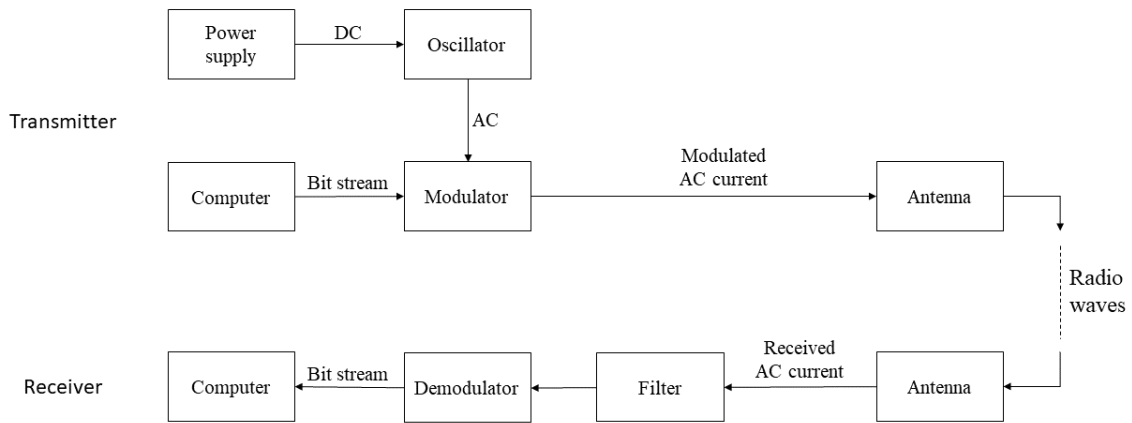
Figure 4.1: Block diagram of the transmission and receiving process in a digital communication system.

At the receiver, the process described above is reversed. From the receiving antenna, the current generated from the electromagnetic waves are amplified and filtered. Filters have a number of purposes, such as removing noise and tuning (i.e. bandpass). The filtered signal is then demodulated, meaning it is converted back into binary values, and transmitted onwards to an output destination.

4.3   Modulation & Demodulation

This section explains in detail the functionality of modulation and demodulation. It also shows the concept of how bit errors occur, which eventually leads to frame errors and packet drops. The aim is to show how bits are handled when going through the physical layer of the OSI model.

Modulation is the process of converting a binary data stream into an analogue signal. This is done using various techniques, depending on the transmission medium, channel quality, requirements and expectations, among others. One of the most basic of modulation techniques, or modulation *schemes*, is pulse amplitude modulation (PAM). In this scheme, only the amplitude of the electrical current is manipulated

based on the input data. The simplest example is 2-PAM, in which there are two levels
of amplitude the signal can represent. In this section, the term "signal" refers to the
electrical current outputted by the modulator, not the radio waves themselves. In 2-
PAM, a binary 1 will often be represented by an amplitude of 1, while a binary 0 will be
represent by an amplitude of -1. These representations are called *symbols.*

A 2-PAM modulator works by taking a binary stream of ones and zeros, and com-
bining them with the current from the oscillator. The output will be an AC where the
amplitude shifts between 1 and -1, depending on the input binary stream, which is ap-
plied to the antenna. At the receiving end, the antenna convert the radio waves into an
electrical current, which will have an amplitude of either 1 and -1. The demodulator
will then be able to convert it back into binary values. Similarly, 4-PAM allows for 4
levels of amplitude, making a single symbol able to represent 2 bits. The efficiency of a
modulation scheme can be measured by *bits per symbol*, meaning how many bits one
symbol is able to represent. Table 4.1 shows how each symbol received in a 4-PAM sys-
tem, will be demodulated as at the receiver. These are called the *symbol translations*,
or a modulation dictionary.

Symbol	Bit translation
3	11
1	10
-1	01
-3	00

Table 4.1: Bit translations for a 4-PAM system.

As mentioned, the transmitted signal level is often referred to as a symbol, where
the symbol represents one of the four bit combinations above. By doubling the amount
of amplitude levels, one doubles the overall bit rate of a system. The amount of ampli-
tude levels varies depending on the demand and what the channel allows.

In both fixed and mobile communication systems, a commonly used modulation
scheme is quadrature amplitude modulation (QAM). In QAM, the signal is modulated
in both amplitude and phase, in order to represent more symbols thus increasing the
number of bits per symbol. This means that each symbol is a unique combination of a
specific amplitude and phase. A regularly used scheme in LTE is 64-QAM, where there

is 8 amplitude levels and 8 phase shifts. By using 64-QAM, one is able to represent 6 bits with each symbol.

In demodulation, the receiver uses the same symbol translation dictionary as the transmitter for interpretation. Because a channel is never ideal, meaning there will always be some form of noise, it uses thresholds on the received signal level with equal spacing between the translations. An example of thresholds used by a demodulator in a 4-PAM system is shown in table 4.2.

Symbol	Threshold
3	$(2, \infty)$
1	$(0, 2)$
-1	$(-2, 0)$
-3	$(-\infty, -2)$

Table 4.2: Thresholds for a received 4-PAM symbol.

From the table, it is understood that if the signal level is above 2, it will be demodulated as a 3. If the signal level is between 0 and 2, it is demodulated as a 1, and so on. The symbols are then demodulated using a dictionary like the one in table 4.1. The assignment of a perfectly round number is arbitrary. This is because in practice, one will never receive a perfect signal level of exactly *"0"*, meaning the limits can be given as "above zero" for a 1 symbol, and "below zero" for a -1 symbol.

4.4   ISI & Bit Errors

Multipath fading occurs when a transmitted symbol reaches the receiver via multiple paths, and therefore at different times because of the difference in length. When a symbol arrives late enough to interfere with the next symbol in line, we get intersymbol interference (ISI). The amount of ISI most often depends on the reflected radio waves' strength and phase offset, but there also several other factors. The following section will go through an example of why a link might fail due to ISI. Examples of multipath fading happening in real networks is shown in sections 6.2 and 6.3.

To show the principle of bit errors, following paragraphs will walk through an example of a 4-PAM system affected by multipath interference. For demonstration purposes, the example holds the following assumptions:

- The difference in length between the direct- and the reflection path correlates to a 360°phase shift of the reflected radio wave.
- The reflection surface is 99% reflective.
- No symbols have previously been transmitted in the system.

Table 4.3 shows the bit stream to be transmitted through the system.

Bit stream	1	1	0	0

Table 4.3: Bit stream to be transmitted through the 4-PAM system.

Using the bit translations in table 4.1, these bits are modulated into the symbols *3* and *-3*, as shown in bold text in table 4.4, and transmitted.

Bit stream	1	1	0	0
Transmitted symbols	**3**		**-3**	

Table 4.4: Symbols modulated from the bits in table 4.3

Assuming the symbol is transmitted through an ideal channel, the first symbol is received and demodulated correctly. However, as the second symbol is received, the reflected radio wave of the initial symbol also reaches the receiver. As shown in the equation for the received signal, 3.7, the receiver will observe a signal amplitude equal to the sum of the two symbols, as a result of the 360 °phase shift. This results in a received signal amplitude of just below 0, because of the small refraction loss during the reflection. Following the symbol thresholds in table 4.2, the receiver will ultimately see the symbols shown in bold in table 4.5.

Bit stream	1	1	0	0
Modulated symbols	3		-3	
Received symbols	**3**		**-1**	

Table 4.5: Received symbols after being affected by ISI.

Using table 4.1 again for bit translations, the demodulator will translate the symbols into the bits shown in bold in table 4.6.

Bit stream	1	1	0	0
Modulated symbols	3		-3	
Received symbols	3		-1	
Received bit stream	**1**	**1**	**0**	**1**

Table 4.6: Received bit stream. Bit error is highlighted.

Comparing the transmitted- to the received bits, we notice there has occurred an error in the last bit. This is called a "bit error". Bit errors occur regularly in any communication system, but the quantity depends on the quality of the channel. Bit errors are usually fixed by implementing "bit error correction" (BEC) methods, which is explained in the following section.

4.4.1 Bit Error Correction

As the name implies, BEC is a method of ensuring the bit streams transmitted match the ones received. This section gives a general description of how BEC methods operate and how they play a role in the overall data rate.

BEC is accomplished by encoding the data bits which are to be transmitted. There are two types of error correction methods: Forwards error correction (FEC) and backwards error correction (BEC).[1] Both of these work by transmitting redundant bits, in addition to the data bits. In FEC, redundant bits are transmitted for the purpose of both noticing bit errors and correcting them. In BEC, the redundant bits are only used to test for bit errors, and if one has occurred, the transmitter is notified and retransmits the stream. While BEC can be viable in a communication system where there are extremely few bit errors, it is generally not used in practice. The trade-off in FEC is whether the redundant bits will provide overall higher data bit rate, rather than retransmitting the bits in the case of a bit error. The difference between *data bit rate* and the *bit rate*, is that in the data bit rate measurement, only bits containing information are counted. In total bit rate, every transmitted bit is counted and included in the statistic.

---

[1]In this section, the "BEC" acronym has two meanings. Its use for "backwards error correction" will only be used in this paragraph.

The bit rate will therefore always be larger than the data bit rate.

Some techniques of FEC coding are convolutional code, low-density parity-check (LDPC) code and turbo coding. Most coding methods consist of compiling a series of bits into a "block".[2]. Many coding techniques use interleavers, which shuffles the order of the bits inside a block, often in a pseudo random fashion. The objective of the interleaver is to separate potential bit errors, as they will most often occur in short bursts.[3] In fixed systems, the BEC and modulation schemes are determined by the signal-to-noise ratio (SNR). This is to ensure acceptable bit error rate (BER) levels, and therefore maximum data rates. The functionality of dynamic schemes are explained in section 4.4.3. The following section, 4.4.2, shows the relationship between the amount of bit errors and the reported SNR.

4.4.2 Bit Error Experiments In Matlab

For further clarification, this section tries to show the relation between the BER and channel quality. The section comprises of two Matlab experiments: Received signal constellation over an AWGN channel and graphs of the symbol error rate (SER)[4] versus SNR.

As a channel quality is degrading, i.e. the SNR decreases, the noise will cause more variations in the signal amplitude and phase, thus making the receiving end more prone to bit errors. Figure 4.2 shows the received signal constellation for a 64-QAM system, with two different SNR settings: 7 dB and 11 dB. The signal constellation was created by a Matlab simulation. The simulation worked by generating 100000 bits, which were then modulated with a rectangular QAM modulator. Following the modulation, AWGN was added to the symbols and graphed in a scatterplot, representing the signal constellation.

---

[2]Normal block sizes are 32 or 64 bits, but this will vary depending on the amount of expected bit errors, and the coding technique

[3]A decoder is designed to only work if the bit error is singled out amongst correct bits, i.e. several, reoccurring correct bits, followed by a single bit error, then several correct bits before another error.

[4]The symbol error rate is the rate at which a transmitted symbol does not match the one received. This is explained later in the section.
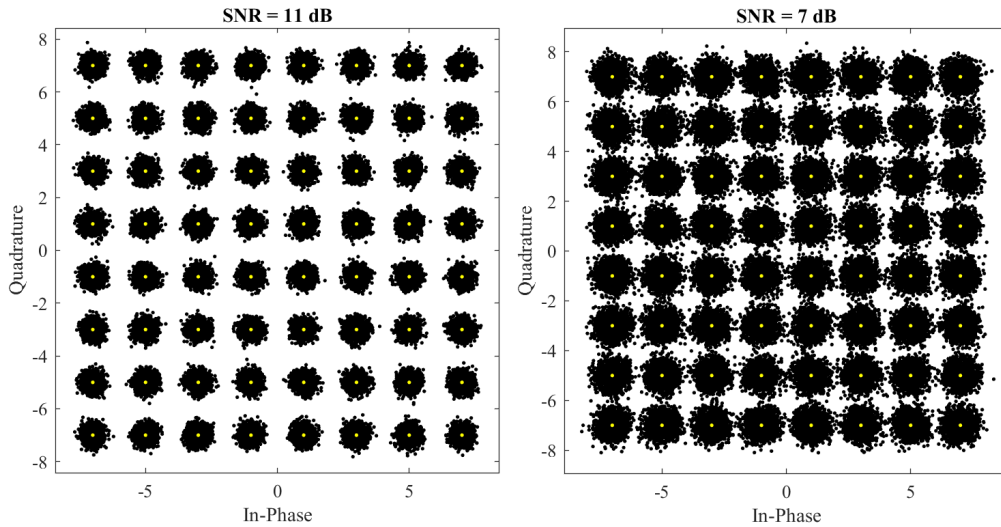
Figure 4.2: Signal constellation at the receiving side for a 64-QAM system with two AWGN channels of different SNR.

The black dots in the figure represents each symbol's amplitude and phase after being applied AWGN. From the graphs we see that as the SNR decreases, or noise increases, the variance of the received amplitude and phase increases. Therefore, as the SNR decreases, symbols are more likely to me wrongly demodulated.

The same principle can also be visualized with graphs of the BER or SER. The difference between the two is that multiple bit errors may occur for the same symbol, but the amount of symbol errors will still only be one. A SER plot graphs the expected SER against the SNR of the channel. The SER is heavily dependent on the modulation scheme. To visualize how the SER correlates to the SNR, figure 4.3 shows the results of a Matlab simluation. In the experiment, bits are generated and divided into four separate sets. Each set is modulated with a different modulation scheme, in this case: Quadrature phase-shift keying (QPSK), 16-QAM, 64-QAM and 256-QAM. The simulation goes through SNR values 0 to 30 dB, and runs until 50 bit errors occur for each SNR value. The error rate is calculated by dividing the 50 bit errors with the total transmitted bits. As with the previous experiment, the simulated channel only applies AWGN.
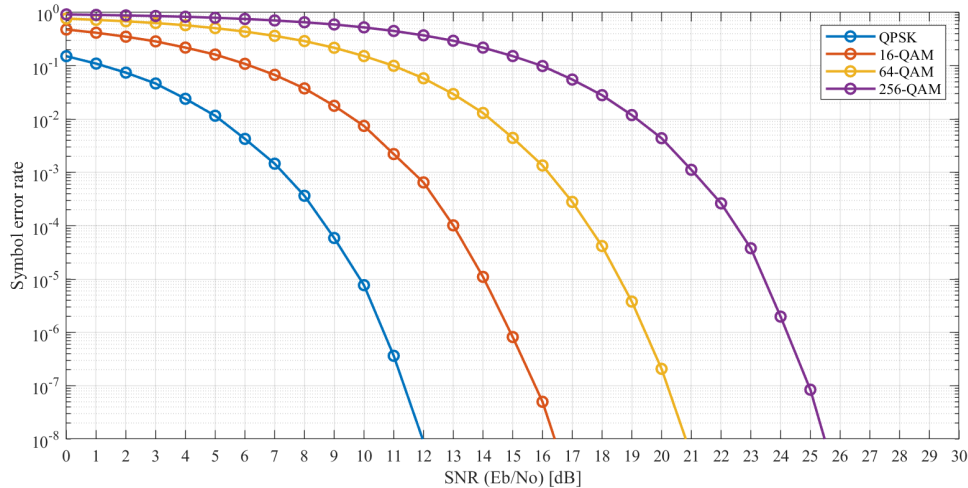
Figure 4.3: Symbol error rate graphs of different QAM orders, over a simple AWGN channel.

The graph tells us that QPSK is less prone to bit errors than 16-QAM, 64-QAM and 256-QAM systems. For examplem a 256-QAM system with a 10 dB SNR channel will have a very high SER, rendering it practically unusable. For the same SNR channel, a QPSK system will have a SER around the order of 10^{-5}, meaning a symbol error will only occur one every million transmitted symbol. This difference is because more levels in phase and amplitude means there will be more symbols for the demodulator to distinguish between.

4.4.3 Adaptive Coding & Modulation

Section 4.4 explains the principles around modulation and coding of the binary data streams. This subsection gives a brief introduction to the topic of adaptive coding and modulation (ACM). In short, ACM provide the opportunity to change the modulation and coding schemes dynamically, based on the channel quality.

ACM is highly attractive because it provides optimal utilization of the link/channel. As mentioned in the previous subsection, the BER depends heavily on the modulation scheme, but also the channel coding technique. In order to minimize the bit errors and retransmissions, ACM controls these schemes based on the SNR. As the SNR decreases, it demotes the scheme. The object of the ACM is to achieve a satisfactory BER, thus ultimately limit retransmissions.

In order to choose the optimal scheme, the radio link equipment uses a modulation table and selects a scheme based on the SNR. Table 4.7 shows an example of how a modulation table might look.

Modulation	Data/redundancy ratio	SNR
BPSK	1/2	0-2
QPSK	1/2	3-5
QPSK	3/4	6-8
16-QAM	1/2	9-12
16-QAM	3/4	13-16
64-QAM	2/3	17-20
64-QAM	3/4	21-24
64-QAM	5/6	25-28
256-QAM	3/4	29-30
256-QAM	5/6	30+

Table 4.7: Example of a modulation table based on SNR with a modulation range from BPSK to 256-QAM.

The table shows which modulation scheme is chosen for some given SNR ranges. It also shows the amount of data bits relative to the total bits transmitted.

A commonly used "lowest-tier" modulation scheme is binary phase-shift keying (BPSK). This is because BPSK is highly resistive against noise, especially amplitude noise. It is also a *binary* modulation scheme, meaning there are only two possible symbols, (statistically speaking) making the BER unable to go above 0,5. Similarly, if the channel quality improves, the modulation scheme is changed again to support more bits per symbol, therefore increasing data rates.

4.5 Diversity

Diversity is an architecture in which multiple channels are used for the same communication link. As as mentioned in section 2.3, diversity has multiple purposes, such as increasing the available bandwidth of the link and providing redundancy. Their main functionality, however, is to provide the receiver an extra set of reference signals for the demodulator. This section covers some of the main diversity options for fixed systems.

As discussed in section 2.4, radio waves are vulnerable to several types of interference and noise. For maritime radio links, multipath fading is a large issue, due to the highly reflective ocean surface. Diversity combats this by transmitting the same data in different ways. For example, the amount of field strength absorbed by the ocean surface varies with frequency. By transmitting the data on two different carrier frequencies, the received field strength will be different for each frequency. Thus, the link is more likely to stay healthy through frequency-selective fading. Similar, for flat fading, the channels may be damaged at different times. This is highlighted in figure 4.4, which shows the received signal power for two channels on a radio link with space diversity, during flat fading.
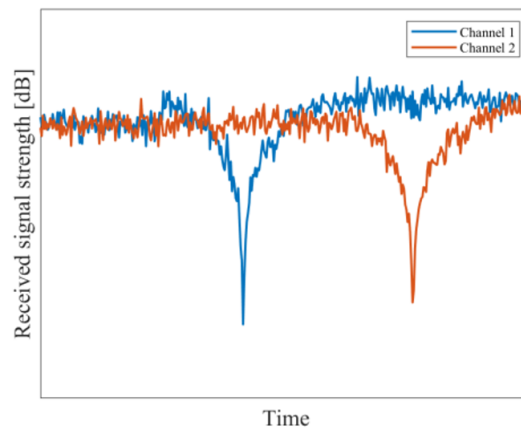
Figure 4.4: Symbol error rate graphs of different QAM orders, over a simple AWGN channel.

From the figure, we see that even when one of the channels are down, the link as a whole will remain stable, as the channels are not down at the same time. There are several types of diversity techniques one can implement, in order to minimize transmission errors. Table 4.8 gives an overview of some common schemes.

Diversity scheme	Summary
Space/antenna	Multiple antennas for the same communication link. An example of this is shown in figure 2.2.
Frequency	Transmitting the same data on two or more carrier frequencies, as described in the example earlier in this section.
Angle	Subdivision of space diversity. Two or more antennas in the same link, each pointed in a different direction.
Polarization	Transmitting on two or more antenna polarizations, i.e. vertical, horizontal, circular, elliptical, etc.
Path	Multiple paths to the receiver, meaning the traffic can go through different routes. This scheme requires additional, available nodes.

Table 4.8: Short overview of commonly used diversity schemes in LOS radio links.

There are advantages and disadvantages to every scheme. A disadvantage of many diversity schemes is that one needs more antennas, which increases both installation, operation and maintenance costs. With angle diversity, there is also the issue of correct alignment. The secondary path also requires a sufficient reflection component, so that the waves can be recognizable at the receiver. Polarization diversity has the additional issue of depolarization. As mentioned in section 3.6.1, depolarization arises when there is a large presence of hydrometeors in the communication system. Path diversity can be hard to implement, as the travel time difference between the two paths increases the difficulty of synchronization the received signals.

Chapter 5

Mobile Communication Systems

This chapter gives an introduction to mobile communication systems and its technical foundation and background. The LTE coverage in the North Sea is continuously expanding, as a result of the increasing demand of a low-latency communication for rigs and vessels, something VSAT cannot provide. As a provider and operator of an offshore LTE network, it is therefore important for Tampnet's NOC employees to have some knowledge of what they are maintaining and operating. This chapter is to serve the purpose of explaining the infrastructure of cellular networks and some of the physical- and data link layer technologies behind LTE.

5.1   Introduction To Cellular Systems

A "cellular network", or a "mobile network", is a network architecture in which the network is wirelessly distributed by multiple base stations. Unlike point-to-point communication, mobile communication systems are classified as point-to-area. Structurally, point-to-area systems involve one antenna connected to several devices, each located (to an extent) arbitrarily within a specific area. The aim is to provide a wireless connection to highly mobile devices or units, making them able to move freely within any of the base station coverage areas.

5.1.1   Cellular Network Generations

For background purposes, this section gives an overview of the history of cellular technologies. The overview consists of a small introduction to ITU and the cellular network generations up to 5G.

Because of continuous advancements, cellular network technologies have developed in generations. The first generation was introduced in the mid 1980s, and the technology quickly advanced. As of January 2018, there are four generations of cellular network technologies, each with their own set of bandwidth capability requirements. These "generations" are specified by the ITU and are solely a set of data rate requirements, and does not come with any solutions or recommended protocols. The generations are set to drive technology forward and for users to know know which data rates to expect. The current generation, 4G (Forth Generation), which was first published in 2008 by the ITU, has a bandwidth requirement of 100 Megabits per second (Mbps) for highly mobile devices and 1000 Mbps for low mobile devices [18].[1] For reference, 3G did not have this clear requirement, however early versions of 3G promised data rates between 348 kbps for highly- and 2 Mbps for low mobile devices.

The fifth version of cellular technologies, 5G, is currently being developed by several private companies. Qatar based telecommunications company Ooredoo, became the first company to launch a commercial 5G network, which opened in May 2018 [20]. In terms of the physical layer, the largest technology advancements in 5G will be higher frequency bands, more bandwidth and greatly increased multiple-input and multiple-output (MIMO) utilization.

5.1.2   Variants of Cellular Infrastructures & Channels

The cellular coverage is continuously expanding in cities across the world, rural areas, in addition to oversea. Each environment comes with a different set of challenges. This section explains some of these challenges for three types of environments: Urban, flat/rural land and oversea/maritime.

---

[1]The actual achievable uplink and downlink data rates are separated into different categories, which depend on the equipment specifications [19]

Urban environments consists of dense buildings, large structures and highly mobile users. There is also plenty more users overall. Because of the densely built obstacles, the transmission is dependent on reflections, diffraction and scattering to maximize coverage. To account for the amount of users, base stations in urban areas often need to be densely built, to limit the amount of users per cell. This can be accomplished by "cell-splitting" and "sectorization". Cell-splitting is the process of dividing a single cell into several smaller cells. This is solely used in urban areas, and will therefore not be explained further in this thesis on offshore communications. Sectorization means that the coverage of a base station is provided by several directional antennas, instead of a single omnidirectional antenna. Each base station, or cell, will then have three sectors, meaning three antennas per cell per frequency band.

In terms of cellular coverage, offshore environments, which is the topic of this thesis, is more comparable to flat, rural areas, than urban environments. In these environments, each cell has very high coverage area, and will most often serve fewer user equipments (UE) per cell. This is a good thing from a technical standpoint, as it will reduce the chance of congestion of a cell sector. The difference between rural areas and offshore environments is that the sea water is highly more reflective. There is also more frequent ducting, weather fronts and more extreme weather conditions in general. An upside of offshore propagation is that there are little terrain height variations and limited obstacles. For overview and review purposes, table 5.1 shows a summary of the channel types discussed in this section.

Environment	Amount of UEs per cell	Coverage	Reflectivity	Cell density
Urban city	High	Low	High	High
Semi-urban	Medium	Medium	High	Medium
Flat land/rural area	Low	High	Low	Low
Maritime/offshore	Low	High	High	Low

Table 5.1: Overview of channel type characteristics related to cellular network infrastructure.

A somewhat unique obstacle for offshore environments is the issue of limitations in terms of available base station locations. Base stations should be placed in a static environment so that the antennas are stationary relative to the Earth. Examples of such locations are oil platforms with fixed locations, i.e. platforms for extraction, storing,

processing, etc. of crude oil and gas. Even though the platforms are sparse, careful planning of the locations are needed to provide optimal coverage and minimize interference and unnecessary costs.

5.1.3 LTE infrastructure and architecture

Prior to discussing cellular geometry, it is helpful to know the basics of mobile network infrastructures. Therefore, the physical infrastructure of an LTE cellular network, in addition to the logical network architecture, called System Architecture Evolution (SAE) [21] is explained here, before the LTE section.

Before going into the infrastructure architecture, it is helpful to familiarize oneself with some commonly used terms. Table 5.2 shows an overview of the most important components in SAE.

Acronym	Full name	Description
UE	User equipment	End user equipment. F. ex. smart phone, tablet, modem, etc.
ENB/eNodeB	Evolved Node B	LTE base station equipment. Has several antennas attached to it. Connects the UE to a S-GW.
S-GW	Serving Gateway	Gateway used by the UE to connect to the network. Several S-GWs may be used for a set of ENBs.
MME	Mobility Management Entity	Gives instructions to the S-GW on handling of every UE session.

Table 5.2: Overview of the key components used in SAE and the LTE infrastructure.

In SAE, the eNodeB acts as the access point between a UE and the main network gateway, the serving gateway (S-GW). The S-GW is connected to both the eNodeB and the mobility management entity (MME). The eNodeB is also connected to the MME, which in terms of hierarchy, gives instructions to the S-GW.

In terms of the network infrastructure, each base station has a fixed location, while the end units are mobile. For capacity and reliability reasons, the base stations are most often connected by fibre optic cables, and act as nodes (hence eNodeB). Figure 5.1 shows the physical infrastructure of an LTE network.
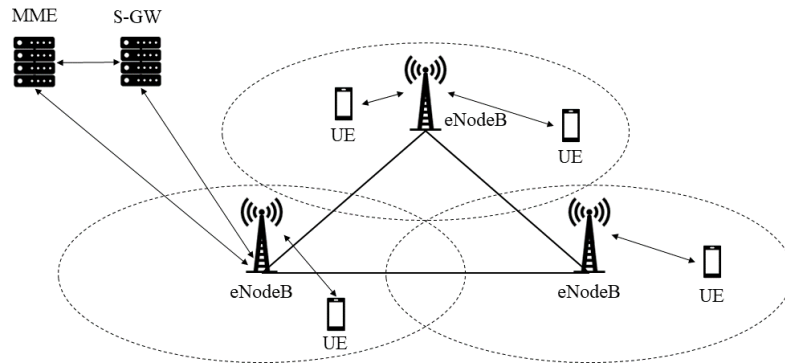
Figure 5.1: Conceptual illustration of the physical infrastructure of a cellular network [4] [7] [8] [9].

The illustration in figure 5.1 shows several UEs connected to three eNodeBs. The thicker lines connecting each eNodeB represents the fibre optic cables. The eNodeBs can also be connected by LOS, provided the risk of environmental effects are satisfactory and the antennas for each communication link are placed in such a fashion that minimizes interference. An LOS link would also require sufficient capacity. Because all external traffic will pass through the S-GW, the same high capacity link between eNodeBs and S-GW/MME is also required. In this illustration, the S-GW is only connected to a single eNodeB, but note that it is possible for the S-GW to be connected to several.

5.2   Cellular Geometry

As explained earlier, a mobile communication network consists of the wireless coverage being provided by several base stations. The infrastructure can therefore be seen as a network of many, individual cells, each providing coverage for a certain area. The use of cellular geometry refers to the principle of planning the locations of these base stations, or cells. By efficient reuse of frequency bands, one enables high utilization of the available frequency band, and thus increasing the capacity of the network. This section explains the principles of cellular geometry and how it may be used to reduce interference.

5.2.1   Inter-Cell Interference

In order to provide total coverage to a certain area, the "footprint" of the base stations will overlap.[2] When two separate base stations use similar frequency bands, it may introduce interference on the channel. We call this "inter-cell interference".

Inter-cell interference occurs because of non-ideal receiver bandpass tuning filters. There are also several other factors, such as non-ideal antennas and environmental factors shifting the frequency. One base station will also provide redundancy by transmitting on two separate bands, e.g. 800 MHz and 1800 MHz. However, this is a non-issue due to the high separation in frequency bands which can be handled by non-ideal filter. On the other hand, two adjacent base stations might have overlapping coverage. To minimize the effects of the inter-cell interference, it is required to carefully plan the locations of each base station. There are two objects in planning a cellular infrastructure: Minimize the inter-cell interference, while also having a high utilization of the available band. This is accomplished by implement frequency planning, with the help of cellular geometry. This enables reuse of the frequency bands, and therefore high utilization.

---

[2]The footprint of a base station is similar to the coverage of a cell. Footprint is a more commonly used term to specify the area vulnerable to interference by the cell.

5.2.2 Structure & Frequency Planning

This section explains the basics of cellular geometry, and how it may be used to combat inter-cell interference. Here, there are a few figures to assist in the explanation of cell footprints and frequency reuse methods.

When planning the coverage area and network infrastructure, each cell is drawn as a hexagon. Thus, the coverage can can be drawn without any gaps between each cell. A hexagon also fits the shape of a base station, in that a base station most often consist of antennas being pointed in three directions in order to provide coverage to the area all around it. Figure 5.2 shows the symbol for a single cell in a mobile network.
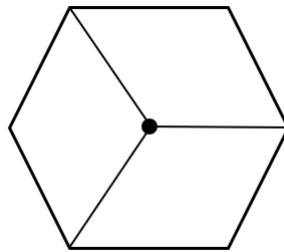
Figure 5.2: General symbol for a single cell in a cellular network. This cell consists of three sectors.

The three sectors represent the cell footprint, i.e. the cell coverage provided by each of the three antennas per base station. As mentioned, the coverage consists of two separate bands. The base station therefore has two antennas per sector. When planning an infrastructure, these cells are put together in clusters, so that the entire area is covered. Figure 5.3 shows a larger cell infrastructure of a single network.
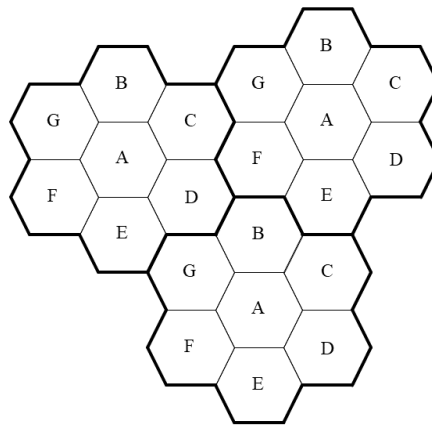
Figure 5.3: Principle structure of cells in a cellular network.

Each letter in figure 5.3 represents one set of transmit and receive frequency band. Each collection of 7 cells, marked with a thicker line, represents a "cluster". In order to avoid inter-cell interference, we therefore require 7 separate bands. Each cell marked with the same letter will not have any overlapping of footprints. This means that a single unit will not be able to adequately hear two base stations with the same set of bands at the same time. Therefore, cells with the same letter are able to use the exact same frequency band, while avoiding inter-cell interference. In this example, each cell marked with the same letter are known as "co-channels", in that it is assigned to the same set of bands. Therefore, if one was to expand the coverage in the network in figure 5.3, one should connect another cluster equal to the others.

However, this will only get you "so far". Regardless of the distance, the receiver will still somewhat be able to hear other base stations operating at the same frequency. This is called co-channel interference (CCI).

5.2.3 Example Of Inter-Cell Interference

Figure 5.4 shows an example of how inter-cell interference may interrupt a communication link. In this example, the UE switches to a separate cell to avoid the interference completely. The figure consist of three graphs. The upper graph shows the "physical cell identifier", meaning the serving cell, i.e. the cell that the UE is connected to, which is shown in blue. The middle graph shows the reference signal received power (RSRP)[3]

---

[3]The terms *RSRP* and *RSRQ* are LTE specific measurements, and explained in section 5.3.1.

for the currently serving cell, in addition to second-best RSRP to another base station. The lower graph holds the same principle as the middle graph, but for the reference signal received quality (RSRQ).
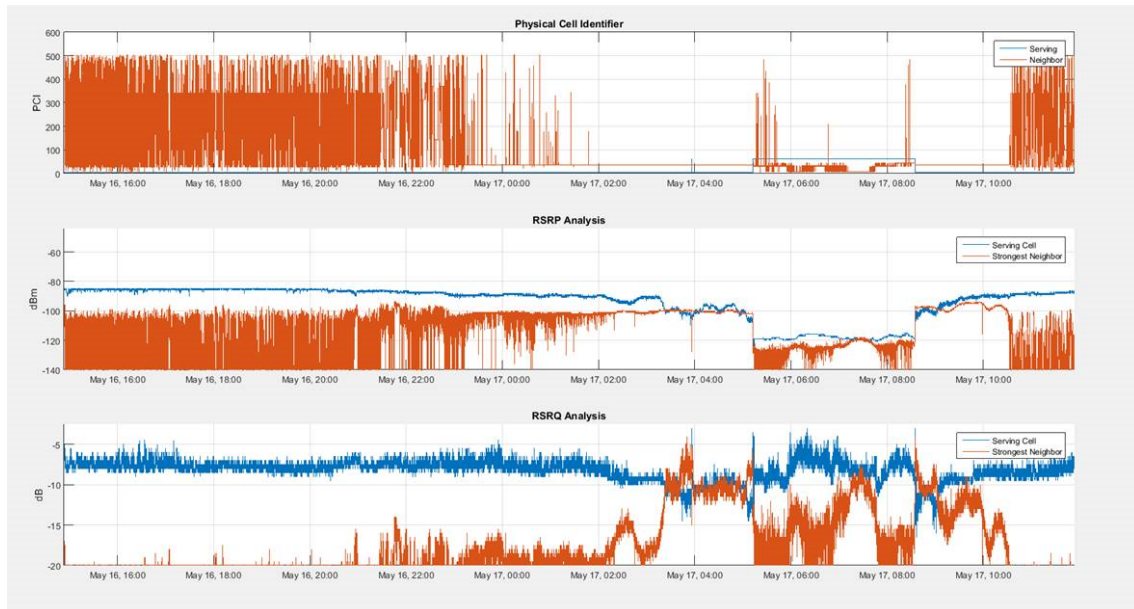
Figure 5.4: RSRP and RSRQ levels during a case of inter-cell interference.

As seen in the upper graph, the UE switches the serving base station around 05:00. The reason for the switch is that the RSRP to the neighbouring cell steadily increases, while the serving cell RSRP decreases. As they approach the same level, the UE tries to avoid the interference by switching to another cell on a different frequency band. This results in the RSRP dropping drastically, as seen in the middle graph. The RSRQ does not decrease, because the received signal strength indicator (RSSI) drops in the same order as the RSRQ. When the interference passes on the previous cell, it switches back, and the RSRP returns to its normal level.

5.3 LTE Systems

LTE is a cellular network "standard". By standard, we mean a set of technologies which when combined, enables high data rate communication.[4] LTE is marketed as a 4G standard, meaning that ITU allows LTE to be labelled a 4G technology. LTE was developed by the 3rd Generation Partnership Project (3GPP) and publicly introduced in 2008, as "LTE 3GPP release 8" [18]. At the time of initial release, it held the following specifications [18]:

- Support of channel bandwidths between 1,4 MHz and 20 MHz, resulting in a maximum spectral efficiency of 15 bps/Hz.
- Option for both time division duplex (TDD), frequency division duplex (FDD) and half-duplex FDD.
- MIMO downlink, with OFDMA channel access.
- Single antenna uplink, with single-carrier frequency division multiple access (SC-FDMA) channel access.
- Optimized for units moving at speeds 0-15 km/h. Support of communication with units travelling at speeds up to 350 km/h.

The frequency bands designated for LTE are situated in the ultra high frequency (UHF) radio band of the electromagnetic spectrum. In Europe, the most common LTE frequency bands are 800, 1800 and 2600 MHz.

5.3.1 Signal Strength & Quality Measurements

This section describes various methods of signal- and channel measurements used in LTE. These measurements are continuously performed by the UE, so that it may choose the best alternative in serving base station, and optimal throughput based on the channel conditions. The action of switching the serving cell is called a "handover". Table 5.3 gives an overview of some measurement techniques.

---

[4]"High data rate" is a very relative term, and changes with technology advancements and commercial expectations. However, at the time of publication, a new standard does provide high data rates.

Measurement technique	Summary
RSSI	Average total received power of every OFDM symbol, meaning every active subcarrier.
RSRP	Average received power in the subcarriers containing a part of the reference signal.
RSRQ	Calculated from the amount of Resource Blocks, RSRP and RSSI. Gives an indication of the received signal quality.
SNR/SINR	The amount of signal power relative to the noise power.
CQI	An indicator of the channel quality, calculated and reported to the network by the UE. Determined by the SNR. Decides modulation order.

Table 5.3: Various signal- and channel measurement techniques used in LTE.

For giving a general idea of the signal strength and quality, RSRP, which is unique for LTE, is often a more accurate measurement than RSSI. RSSI counts the total received power, which includes signal power from non-serving cells and other sources. RSRP counts only the average received strength on carriers used by the relevant UE, meaning it excludes interference as signal strength.

RSRQ takes both RSRQ and RSSI into consideration, in addition to the amount of resource blocks (RB) the RSSI is measured over.[5] The RSRQ formula is given by equation 5.1.

$$RSRQ = \frac{N \times RSRP}{RSSI} \tag{5.1}$$

where:

N is the amount of resource blocks used for measuring RSSI.

An an example, assume the RSRP remains static while RSSI increases. This will mean that while the received signal strength is increasing, it does not contain any data and is most likely noise or interference. Increased noise and/or interference will naturally decrease the quality of the signal, which we see is the case in equation 5.1.

---

[5]Resource blocks are explained in section 5.3.2.1.

SNR is the power of the received signal, relative to the power of the received noise. However, if assuming equal distribution of transmitted symbols, the mean symbol value will be 0. By also assuming a zero-mean noise addition, the SNR can be given by the variance of the symbol amplitude distribution, relative to the variance of the noise distribution. This form is shown in equation 5.2, along with its often used decibel form in equation 5.3.

$$SNR = \frac{\sigma^2_{signal}}{\sigma^2_{noise}} \tag{5.2}$$

$$SNR_{dB} = 10\log_{10}(\sigma^2_{signal}) - 10\log_{10}(\sigma^2_{noise}) \tag{5.3}$$

where:

σ^2_{signal} is the variance of the symbol amplitude distribution,

σ^2_{noise} is the variance of the noise amplitude distribution.

Similar to SNR, the signal-to-interference-plus-noise ratio (SINR) counts interference as noise. This results in the power, or variance, of the interference being added to the denominator in equation 5.2, or as an additional subtraction in equation 5.3.

Channel quality indicator (CQI) is a value that is calculated by the UE and reported to the eNodeB. The aim of the CQI is to establish a modulation scheme that will result in a block error rate (BLER) not exceeding a given percentage, e.g. 10 or 20 %.[6] The modulation schemes in LTE are 4-, 16- and 64-QAM. [7]. Because there are only three, the rest of the CQI values determine the coding scheme, thus the amount of redundancy bits and spectral efficiency.

The reported CQI depends mostly on SINR, but also the UE specifications, such as antenna diversity scheme and antenna gain. CQI is reported as a 4 bit integer, i.e. between 0 and 15. Depending on the available options for modulation and coding, not all 4 bits are required. Because the CQI determines both the coding and modulation scheme, it has a very high correlation with the achievable data rate of an LTE system.

---

[6]BLER is the rate at which one or more bit errors occurs within bit block. When given as a percentage, it refers to the percentage of encoded blocks containing one or more bit errors. Recall from section 4.3 that coding occurs in blocks for more efficient error correction.

[7]4-QAM is the same modulation scheme as QPSK.

5.3.2 LTE In The Physical Layer

This section gives an overview of how LTE operates in the physical layer. Because LTE has slightly different design for uplink and downlink, the section is divided into two subsections. The first describes the downlink design, while the second describes the uplink.

5.3.2.1 Downlink Transmission

For downlink, the peak data rate depends on the diversity scheme. For a SISO link, the peak data rate is 100 Mbps, however by increasing to 2x2 or 4x4 MIMO, it increases to roughly 150 Mbps and 300 Mbps, respectively. [22].[8]

LTE uses OFDMA as its downlink multiple access technique. This scheme is based on orthogonal frequency division multiplexing (OFDM), a multi-carrier modulation (MCM) technique, in which the allocated channel bandwidth is divided into several "subbands", each with its own "subcarrier". The narrowness of the channels make them almost ideal, and therefore much less vulnerable to frequency selective fading as a result of, amongst others, multipath fading. Each subcarrier is modulated with a bit stream of low bit rate. This helps limit the ISI, while still providing high overall data rate, due to amount of subchannels used simultaneously. Another feature in LTE which reduces ISI is "cyclic prefix". To combat inter-carrier interference (ICI), each carrier is placed orthogonally relative to each other. In short, this accomplishes cancelling of ICI, given there is no jitter or frequency-noise in the system.

An OFDM symbol is made by combining each symbol from every subcarrier in the frequency domain, then applying the inverse fast Fourier transform (IFFT) to retrieve the discrete Fourier transform (DFT) samples. These samples make up the OFDM symbol. At the receiver, the fast Fourier transform (FFT) is applied to retrieve the transmitted symbol.

---

[8]These limits are calculated with no regard for encoding. The real peak data rate is therefore somewhat lower.

In OFDMA, each user is assigned a time-frequency resource, called an RB. A single RB consist of 12 subcarriers and a time slot of 0.5 ms. This is a concept similar to TDMA and frequency division multiple access (FDMA), where units are given a time slot, or a static carrier to use for transmission. All subcarriers are shared and new RB are assigned every 1 ms. This assignment is performed by the eNodeB. For a 20 MHz bandwidth, there is a total of 100 RB available for allocation by the eNodeB. The experiments in section 5.3.4.2 shows how the downlink and uplink throughput correlates to the amount of allocated RB.

5.3.2.2   Uplink Transmission

As mentioned in the previous section, the UE is allocated RB by the eNodeB. Table 5.4 shows an overview of how the subcarriers in the RB are allocated in uplink, along with a short description of each subchannel type.

Subchannel name	Acronym	Summary/purpose
Physical uplink shared channel	PUSCH	Data transmission by the UE.
Physical user control channel	PUCCH	Transmission of control information, i.e. CQI, MIMO feedback, scheduling requests, among others.
Physical random access channel	PRACH	Used for initial contact with the eNodeB, as the UE requests available PUSCH channels.
Sounding reference signals	S-RS	Used by the eNodeB for channel quality and transmission timing evaluation. RSRP is measured over these subcarriers.

Table 5.4: Overview of the subchannel types used in LTE for uplink transmission.

LTE uses SC-FDMA for uplink data transmission.[9] This is because OFDMA generate signals with great peak-to-average ratio. This means that the amplifiers required for OFDMA need a large dynamic range. This causes them to be quite inefficient and very expensive. However, both techniques are quite similar in architecture. As with OFDMA, SC-FDMA is a MCM scheme, meaning the total channel bandwidth is divided

---

[9]In LTE, only the data transmissions uses SC-FDMA. Control bits are transmitted on OFDMA subcarriers. This is acceptable due to the low amount of control information in relation to actual data.

into several subcarriers. Their difference, however, is SC-FDMA's use of DFT, which is applied between the modulation (QPSK or M-QAM) and the IFFT. The DFT is used to carry the time-domain signal, coming from the modulator, into the frequency domain. The eNodeB assigns each user with a unique set of FT coefficients, i.e. it tells the unit which subcarriers to use for transmission. These subcarriers can be grouped together and seen as one main carrier, hence the name "single carrier"-FDMA.

5.3.3   MIMO Concepts

MIMO is the concept of using multiple transmitter and receiver antennas for the same communications link. Diversity, for example, is a MIMO technology. In LTE, 2x2 is a popular set-up, and a central factor in increasing the data rate. LTE also supports 4x4 MIMO, which increases the bit rate up to 300 Mbps.

For LTE, there are two main options for MIMO: Spatial multiplexing and transmit diversity. In spatial multiplexing, two antennas trasmit different blocks at data. This effectively doubles the bit rate, or optionally the overall capacity of the eNodeB. This is the most popular MIMO option. Transmit diversity is a form of space diversity, as the name suggests. Here, the data is copied onto two different channels which use different coding schemes and subcarriers, but ultimately transmit the same data. Transmit diversity results in redundancy, higher SNR and modulation schemes of higher order, and therefore fewer bit errors and possibly higher data rates.

5.3.4 LTE Lab Experiments

This section demonstrate the results of two experiments conducted in order to find the correlation between RSRP, SINR and other various quality and service measurements. The experiment was conducted for both uplink and downlink with their own results. The experiment results is divided into two sections:

5.3.4.1 Maximum throughput, SINR, QCI and RSSI based on RSRP.

**5.3.4.2** Allocation of RB based on the SINR.

For the first experiment, the downlink results show the correlation between RSRP and the maximum throughput, SINR and QCI. For uplink, the results show the correlation between RSRP and maximum throughput, SINR and RSSI. In the second experiment, the downlink results show the amount of RB allocated for SINR values between -6 and and 30 dB, for some different levels of throughput. The uplink results shows the same, but for SINR values between -2 and 22 dB.

The experiments was performed by transmitting data between two traffic testers, where the traffic was routed through LTE on 20 MHz bandwidth. The first step was therefore to set up an MPLS service going through an LTE network and connecting two SAR-8s. Thereafter, a traffic tester was installed on each end. All the work was performed in the lab of Tampnet's office in Stavanger. Table 5.5 shows the equipment used for the experiment.

Equipment	Quantity
SAR-8	2
EXFO MAX-860G Traffic tester	2
CPE with chipset Sierra MC7304	1
Trilithic Model RSA-35110D-SMA-R Attenuator	1

Table 5.5: List of equipment used for LTE experiments.

Figure 5.5 shows the network topology used for the experiments, with the traffic tester in each end. As noted in the topology, the rightmost equipment is representing the offshore location (platform, vessel, etc.), while the SAR-8 and the traffic tester on the left of the LTE network is representing equipment onshore.
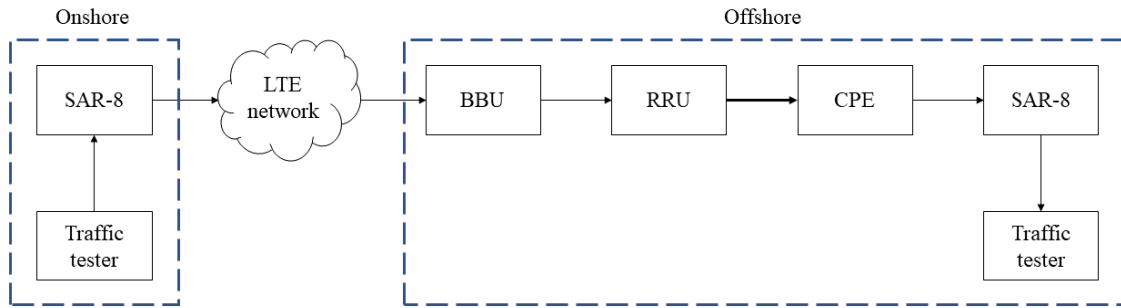
Figure 5.5: Network topology of the LTE experiment.

The attenuator was placed between the RRU and the CPE, as noted with a ticker arrow in figure 5.5. The attenuator was a variable attenuator with a range of 0 - 110 dB in steps of 1 dB. Figure 5.6 shows a photograph of the physical set-up with the traffic testers and the attenuator.


Figure 5.6: Photograph of traffic testers and variable attenuator used for the experiment.

As the experiment was running, the necessary parameters were set on either the attenuator or the traffic testers, and all the data was recorded on the laptops.

5.3.4.1 Downlink & Uplink Throughput Capacity

This section divides the downlink and uplink experiments. The downlink experiment was ran by pushing the maximum amount of traffic for each step in added attenuation, while keeping the radio link control (RLC) buffer stable.[10] For each step in attenuation, we noted the reported RSRP, SINR, CQI and throughput.[11] For downlink, the strength of the reference signals were 18.2 dB. Figure 5.7 shows the results of the downlink test. To show the correlation, each measurement is graphed in the same figure, with three separate y-axes, each with different scaling. The color of each line corresponds to the color of the axis.
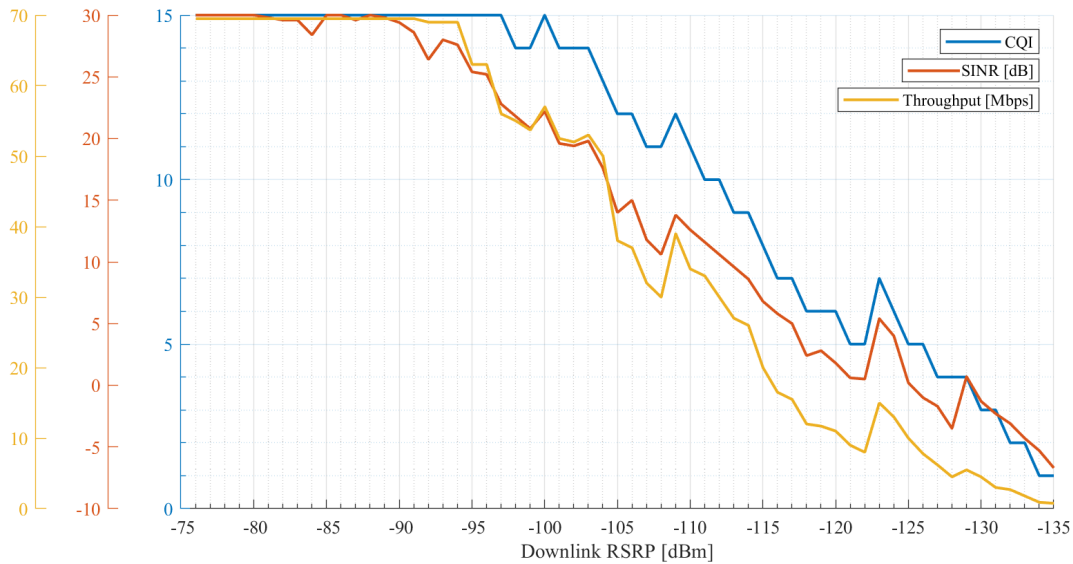
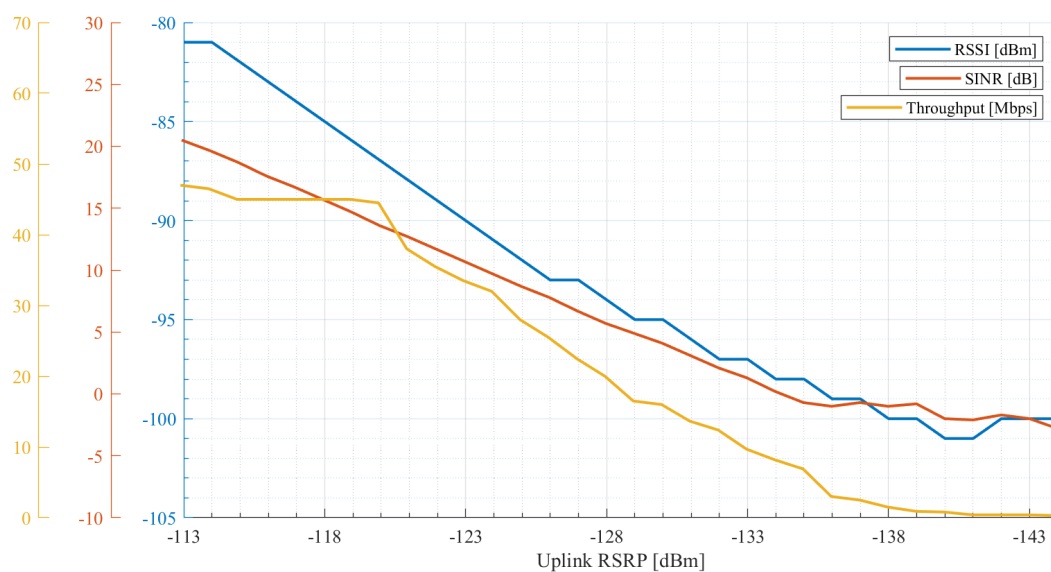**Figure 5.7:** Graph of the downlink throughput, SINR and CQI as a function of RSRP.

The minimum RSRP was -75 dBm, which is why the graphs start at this point. The small spikes at RSRP -100, -109 and -123 dBm are due to a non-linear attenuation decrease, which is a hardware fault in the attenuator. Regardless of this, the graph clearly show the relation of each measurement and the RSRP. As seen in the throughput graph, the maximum was 70 Mbps. This is because the CPE is a category 3 UE. [19] The tests ran until radio link failure, i.e. the link was completely down, which happened at -

---

[10]The RLC participates in ensuring reliable data transfers. The RLC buffer temporarily stores the data to be transmitted, naturally in a "first in first out" fashion. If the buffer gets overloaded, data is dropped at the RLC layer.

[11]Because of 20 MHz bandwidth, there are 100 resource blocks available. We noted both Initial BLER and Retransmission BLER, but Retransmission BLER was a stable zero until the very last step prior to radio link failure.

135 dBm RSRP. As expected, there is very high correlation between the CQI and the throughput.

For uplink, the procedure was the same, however instead of CQI, we noted the RSSI reported by the cell.[12] Also, in uplink the strength of the reference signals were 12,4 dB. This was discovered post experiment. The different reference signal strength cause an offset in the relation between RSRP and SINR for uplink and downlink, but will not change the course of the graphs. Figure 5.8 shows the results of the uplink test. As with the previous figure, the color of the three y-axes corresponds to the color of the lines.

**Figure 5.8:** Graph of the uplink throughput, SINR and RSSI as a function of RSRP.

Because of limitations in the CPE, it did not report RSRP values below -113 dBm, which is why the data starts here. Compared to figure 5.7, there is a clear difference in throughput, because of limitations in the CPE. From the SINR and RSSI, we see that the signal levels reach the noise floor at around -138 dBm RSRP, while the CPE is still being able to handle around 1 Mbps traffic.

---

[12]CQI is a downlink specific measurement, therefore not relevant to the uplink test.

### 5.3.4.2 Resource Block Allocation

For this experiment, we set a fixed attenuation, then steadily increased throughput while logging the SINR and RB usage. The attenuation was incremented by 5 dB each step. For downlink, the RSRP starting points were -80 dBm for downlink, and -100 dBm for uplink. The throughput was tested until the bit flow became unstable. The results show the correlation between the reported SINR and RB usage based on some example throughputs. The results of the downlink experiment is shown in figure 5.9.
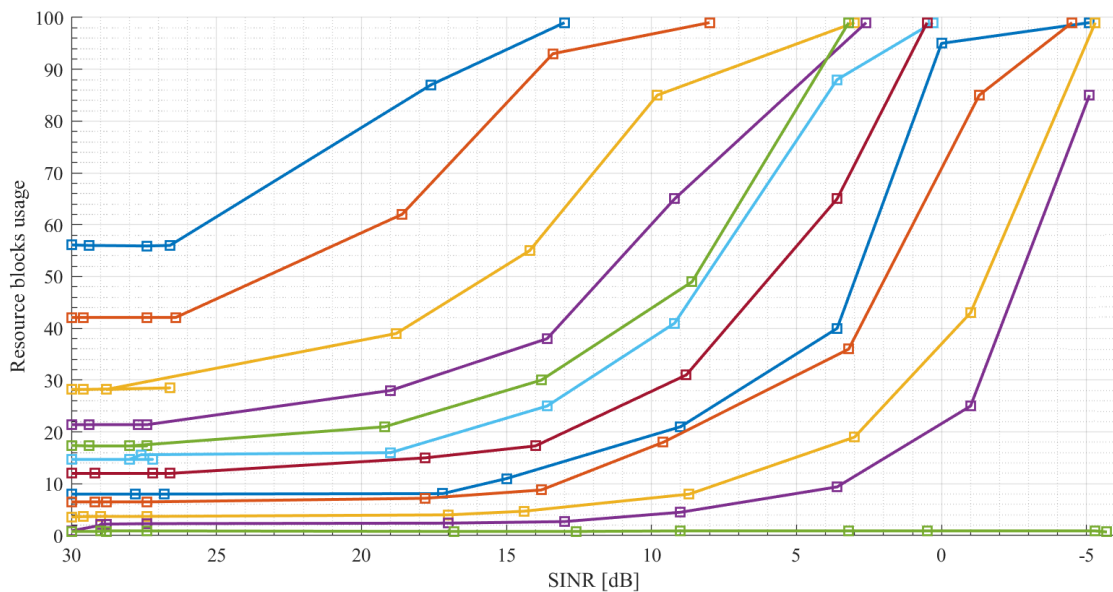
Figure 5.9: Number of allocated RB as a function of SINR.

As the RB usage reaches 99, the bit flow becomes unstable, as the channel cannot handle the throughput because of the channel quality conditions. In other words, the cell does not have the resources to provide the requested throughput when the channel SINR is below a certain threshold. As explained in section 5.3.2, the throughput is heavily dependent on the amount of RB allocations. This is clearly shown in the graph, where the highest throughput has a stable 56 RB allocated during near perfect SINR conditions. As expected, the allocations decrease with throughput demand.

The uplink test results is shown in figure 5.10. Here, the SINR range from -2 to 22 dB. The smaller range is due to limitations in the CPE. The tested throughputs were the same for both downlink and uplink.
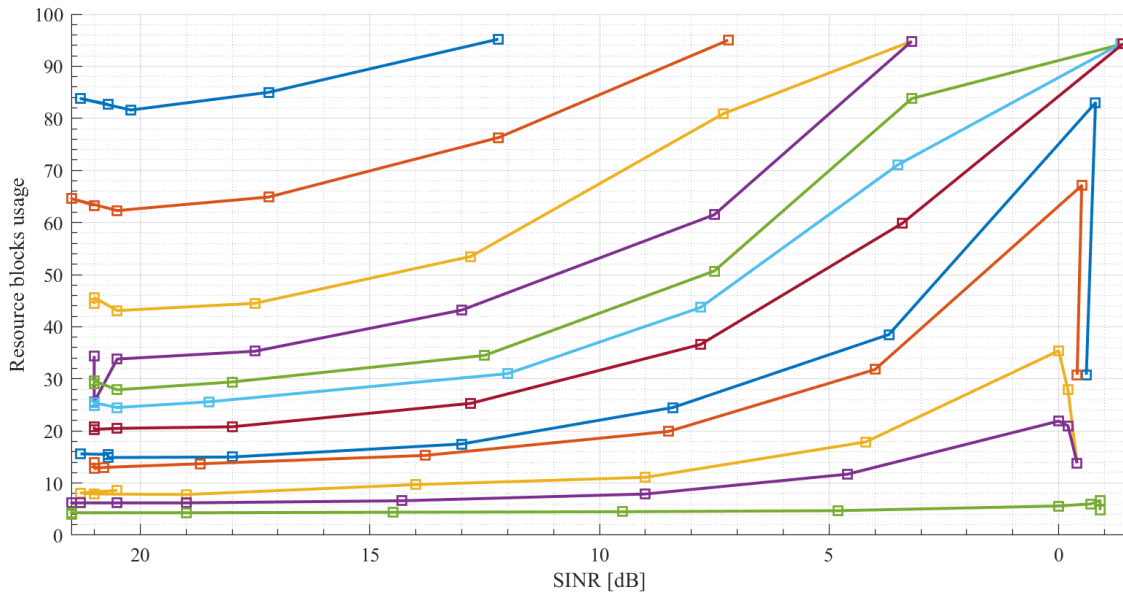
Figure 5.10: Graph of the uplink RB usage as a function of SINR.

As with downlink, the bit flow fails as the RB usage reaches close to 100. The limitations in the CPE capabilities results in a significant reduction in capacity. When the uplink traffic is at its lowest, the RB usage is at a stable 4. These 4 RB are for non-data transmissions, such as the user control channel, PUCCH. For uplink, radio link failure occurred at -1 dB SINR.

Chapter 6

# Examples Of Offshore Propagation Impairments

This chapter describes some special occurrences that happens in offshore environments. Each occurrence is divided into a separate section. Each section consist of a real world example, which has been recorded on the Tampnet network. Some of the occurrences are supplemented with Matlab experiments, showing how the offshore effects can be modelled. Some of the examples are large ships blocking the radio path between two terminals, multipath fading as a result of variations in the refractive index and multipath fading due to tidal variations.

6.1   Line-Of-Sight Obstruction

This first section describes what happens when a large obstacle crosses the LOS path of a fixed communication system. The description is supplemented with an example of a boat crossing a long range radio link between platforms "Tiffany" and "Piper B". Following the example is the results of a Matlab simulation showing the theoretical diffraction attenuation for this system, and shows how it fits with the real-time example.

The diffraction attenuation increases with path distance, because more of the Earth will be inside the Fresnel zone [16]. Alternatively, one can look at this as the radio waves travel closer to the Earth surface. Because of their lower altitude, floating objects on the

ocean surface cause a greater obstruction, therefore increasing diffraction attenuation. The classic example are tall boats crossing the radio link. This happens somewhat regularly, but mostly affect the lower channel. Figure 6.1 tries to illustrate this phenomena [10]. The communication system in the illustration has antenna diversity where the main channel is physically located above the protection channel.
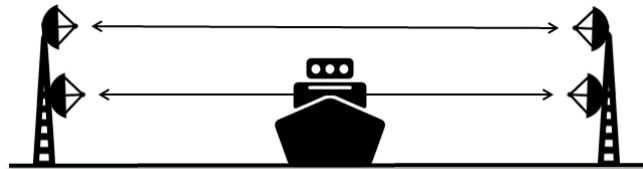

Figure 6.1: Illustration of how a radio link channel can be blocked by an object [4] [5] [10].

The difference in height between the two channels varies depending on the space availability on the platform, but is usually around 10 m.

Because of limitations in achievable antenna height, this occurrence is somewhat common. Following paragraphs will describe a live example taken from an event on 24.04.2015. Here, a tanker called "Elizabeth Knutsen" crossed a between Tiffany and Piper B. The Tiffany - Piper B radio link specifications is listed below.

- Path distance: 59,3 km
- Frequency band: 6 GHz
- Antenna heights: 103 m and 70 m

Elizabeth Knutsen is a 265 m long tanker, with a maximum height of about 50 m. Figure 6.2 shows an image and general information on the vessel in question [23], along with an image of the vessel crossing location.
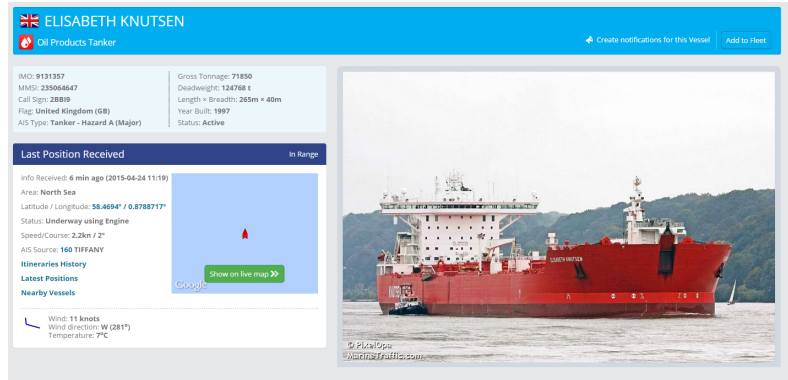
(a) Image of the Elizabeth Knutsen vessel.
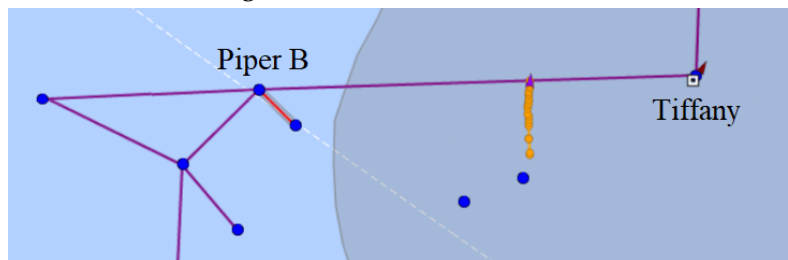
(b) Crossing location of Elizabeth Knutsen.

Figure 6.2: Information on Elizabeth Knutsen, a large vessel blocking the LOS between Tiffany and Piper B.

Because of its size, this type of vessel is more damaging than most. Additionally, as seen in subfigure 6.2b, the vessel crosses near the centre of the propagation path where the radio waves are at their lowest altitude.

The received signal strength on both channels during the crossing is shown in figure 6.3. The graphs only displays the received strength on the Tiffany end, but the pattern was more or less identical on the Piper B end. The data was retrieved at 13:34 and 13:28 on 24.04.2015, respectively.
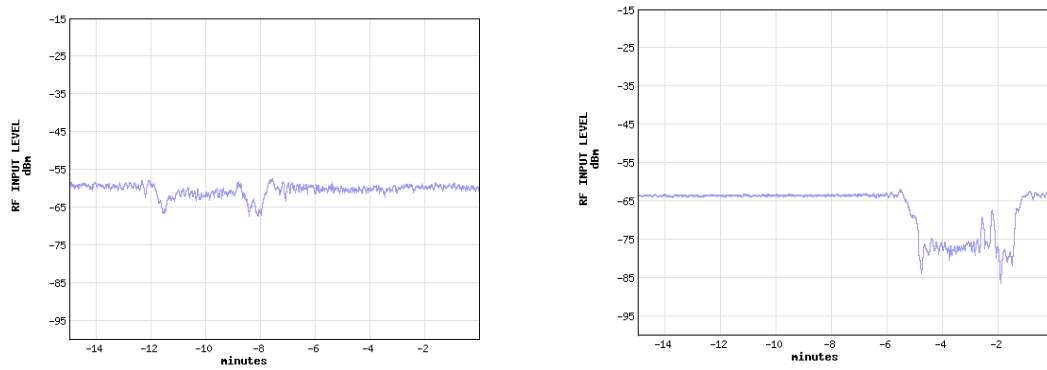
(a) Main channel received signal power.

(b) Protection channel received signal power.

Figure 6.3: Received signal strength on main and protection channel, respectively, on Tiffany end between Tiffany and Piper B during tanker crossing.

From the graphs we see that the protection channel was greatly more affected by the crossing. In subfigure 6.3b, the spikes at the start and at the end of the dip in signal strength are due to the taller structures at the front and at the end. These taller structures are what affected the signal strength in subfigure 6.3a. The flatter area in the middle in subfigure 6.3b is the side of the boat itself, as seen in the image in figure 6.2a. The two spikes in the middle is most likely reflections off the cabin tower, as seen in figure 6.2a.

To see how well this example fits an ITU recommendation on diffraction attenuation, the following paragraph shows the results of a Matlab experiment. The experiment consisted of implementing Recommendation ITU-R P.526-14 [24] into Matlab. The obstacle was modelled after a knife-edge obstacle steadily increasing in height. The system parameters were configured according to the actual radio link, in terms of antenna heights, path distance and frequency. Figure 6.4 shows the results of the simulation. The two markings on the graph shows the attenuation for each channel when the obstruction is 40 m above the LOS of channel 2.
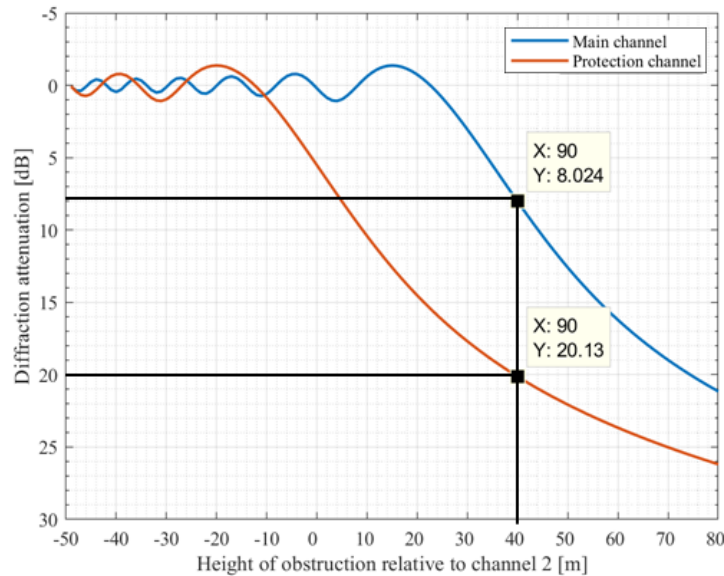
Figure 6.4: Diffraction attenuation for a 59.3 km path. 6 GHz frequency.

The figure shows that as an obstacle is 40 m above the protection channel, the diffraction attenuation is 20 dB. As seen in figure 6.3b, this is highly representative. The same also applies to 6.3a, where we see a 7-8 dB attenuation for the same incident. While these values are quite accurate, it is not likely the obstacle was 40 m above the propagation path of the protection channel. Diffraction attenuation is among the hardest to estimate because of its variance and many parameters, especially for such a long radio link. Some error is therefore to be expected, especially because the formula used in the simulation is meant for knife-edge obstacles.

6.2   Effects of Tidal Variations

This section describes how tidal variations might effect the received signal strength for a fixed system. Following the example is the results of a Matlab simulation, further explaining how a small change in sea level height could affect an entire communication system.

The *tidal range* is defined as the maximum difference in sea level during high and low tide. In the North Sea, the tidal range is roughly 1,5 m. The tide interval depends on a number of factors, but is roughly 12 hours from peak-to-peak high tide. These height changes could drastically change the received signal strength in two main ways:

diffraction and reflection.

The following example is taken from the protection channel of a fixed radio link between the "Fulmar" and "Clyde" platforms, which had periods of intense fading during flat sea periods, where the tidal patterns can be observed. The Fulmar - Clyde radio link specifications is listed below.

- Path distance: 9,3 km

- Frequency band: 7,5 GHz

- Antenna heights: 45 m and 55 m

Figure 6.5 shows the received signal strength of the Fulmar - Clyde protection channel during a 72 hour time period between 08:00 20.06.2015 and 08:00 23.06.2018.
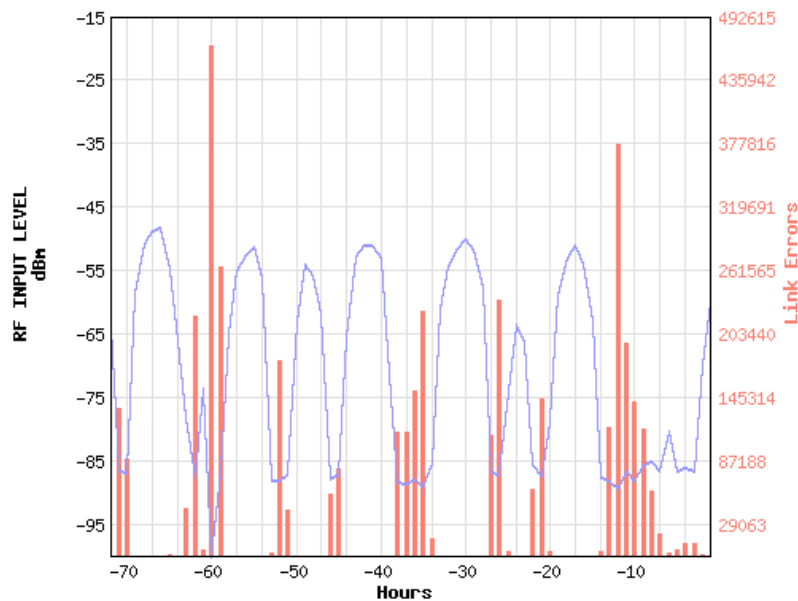

Figure 6.5: Received signal strength on Fulmar end during a 70 hour period on the LOS protection channel between Fulmar and Clyde platforms.

As mentioned, diffraction attenuation increases as more of the Earth enters the Fresnel zone. However, because of the short distance of 9,3 km and decent antenna heights, these variations are not solely caused by diffraction. The red columns represents the amount of link errors for its respective hour. These errors are mostly bit errors. As explained in section 4.3, the BER depends on the SNR, and as the signal levels goes below -75 dBm, errors starts to occur during demodulation. The issue with this

link was the ocean reflection causing multipath fading, as shown in figure 3.9. Because of decorrelation between the heights of the transmitting and receiving antennas, the small change in sea level was enough to cause a 180°phase shift between the direct and reflected radio waves.

To show that the reflection was the issue, we can look at the reflection mean coefficient using the given distance and height above sea level. Figure 6.6 shows the results of a Matlab simulation, using a model of the Fulmar - Clyde radio link. This experiment finds the mean coefficient when the height of the sea level variates between -0,7 and 0,7 m from a reference sea height. In the simulation, the tide changes are represented by a sinusoid function. For accuracy, the period of the sinusoid was set to 12 hours. The communication system geometry was simulated by setting the correct antenna heights, path distance and frequency. Note that this experiment was highly theoretical, as tidal changes are more complex than simply a sinusoid.
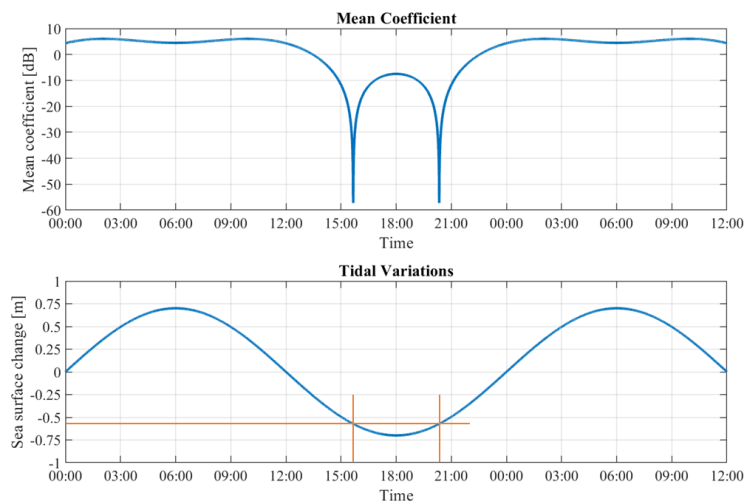
Figure 6.6: Experiment on tidal change effects on a model of the Fulmar - Clyde LOS.

As seen in the figure, the multipath fading occurs when the sea level is close to -0,5 m relative to the reference sea level. In the simulation, the sea level reaches this height two times during the day, at around 16:00 and 20:00. These are marked by the orange lines in the lower graph. This effect, where the low (or high) tide is close to the phase cancellation height, can also be observed in figure 6.5, at hours -60, -25 and -10 hours on the x-axis.

6.3   Effects of Multipath Fading & Atmospheric Ducts

Multipath fading occurs because of the different phase shifts of the reflected path. As the reflection path grows longer of shorter, the electrical field will either add or subtract to the total received field strength. For fixed radio links, the length of the reflection path will increase or decrease depending on the refractive index of the atmosphere.
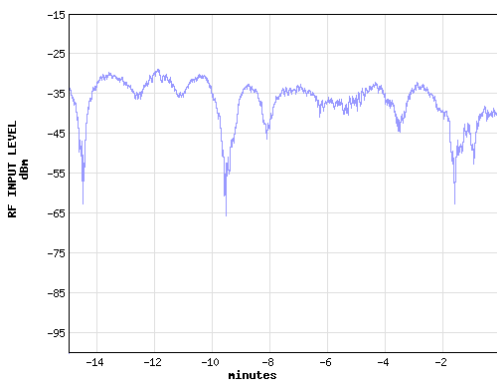
The most extreme change in refractive index is during the event of a surface-based *atmospheric duct*. A duct is a layer highly humid air. Because of its higher density, a duct will cause the radio waves curve more, therefore affecting the length of the reflection path.

Multipath fading can be identified by several gradual decreases of the received signal strength. As seen and explained in figure 3.9, the gradual decrease is due to the length of the reflection path, and therefore the phase offset, continuously increasing. This effect will most often be visible for VHF (and above) systems, as the wavelengths are much shorter and the phase cancellations will be more frequent for a given reflection path length increase.
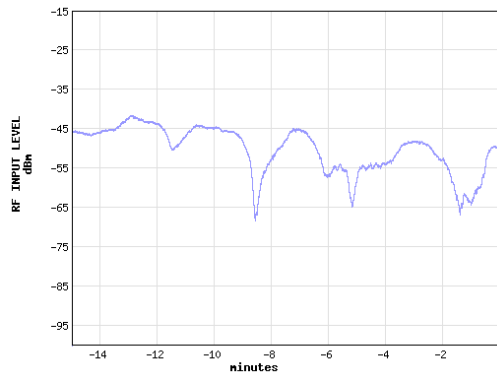
The following page shows three examples of multipath fading. Figure 6.7 show the received signal strength of the fixed radio links with the respective system specifications listed on the right of each graph.
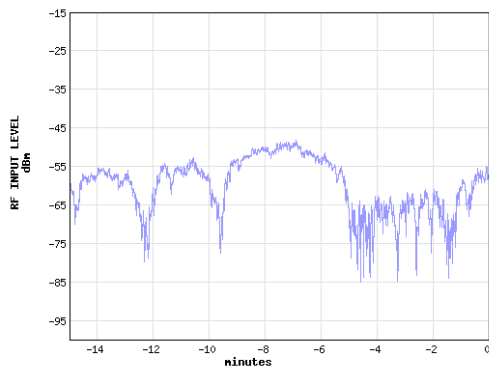
(a) Tartan A - Buchan. Data recorded at 13:14 on 08.12.2016.

Tartan A - Buchan, protection channel.

- Path distance: 51,9 km.

- Frequency band: 6 GHz.

- Antenna heights: 50 m and 60 m.

(b) Tiffany - Piper B. Data recorded at 13:11 on 08.12.2016.

Tiffany - Piper B, main channel.

- Path distance: 59,3 km.

- Frequency band: 6 GHz.

- Antenna heights: 103 m and 70 m.

(c) Valhall - Maersk Resolve. Data recorded at 09:32 on 07.09.2016.

Valhall - Maersk Resolve, main channel.

- Path distance: 35,1 km.

- Frequency band: 6 GHz.

- Antenna heights: 40 m and 30 m.

Figure 6.7: Examples of received signal strength during periods of multipath fading for three 6 GHz fixed links.

Chapter 7

Conclusion & Outlook

This thesis has presented several factors related to power attenuation in wireless communication systems located in offshore environments. Additionally, it provides introductory elements to both fixed and cellular communication systems. The main motivation for this thesis, and for the associated work, was for new employees in the NOC to this paper as a starting point for increasing their competence within these topics. The field of telecommunication is enormous, with a highly steep learning curve. The aim has been to provide sufficient material for readers to understand how the operation ties together with the technologies and environment in the North Sea systems.

The thesis was divided into four main parts: Radio propagation, fixed systems, mobile systems and offshore environmental events. The chapter on radio propagation give an insight into the factors affecting radio waves behaviour in general and in offshore environments. These factors were then connected to ITU-R recommendations, and presented in equations and graphs which displayed their impact. The fixed systems chapter took an introductory look at the structure of microwave links, explaining their function and operation. Similarly, the mobile systems chapter also look at the structure and operation of LTE in the physical layer, in addition to cellular infrastructures. The chapter on environmental events gave examples on some common attenuation factors affecting offshore systems, which has been captured live. All these factors were previously introduced in the chapter on radio propagation. The result has been a document highly useful for both NOC operators and all, complete with technical documents, simulations, experimental results and examples gathered over years of

operation.

Future projects taking this work onwards could build upon this foundation by going deeper into each subject. This could include adding more attenuation factors in the radio propagation chapter and a larger and more complete explanation of fixed and mobile communication systems in not only the physical and data link layers. Provided data is available, implementing more examples of offshore occurrences could also be worth doing.

Bibliography

[1] P. Wormer, "Electromagnetic wave." https://commons.wikimedia.org/wiki/File:Electromagnetic_wave.png, Dec 2010. Image found via Wikimedia Commons. Accessed: 14.06.2018.

[2] Bidgee, "Shrouded microwave relay dishes on a communications tower in australia.." https://commons.wikimedia.org/wiki/File:Parabolic_antennas_on_a_telecommunications_tower_on_Willans_Hill.jpg, Oct 2008. Photo found via Wikimedia Commons. Accessed: 01.06.2018.

[3] M. A. Padriñán, "Communication antenna." https://www.pexels.com/photo/antennas-communication-connection-frequency-579471/, Aug 2017. Photo taken from Pexels. Accessed: 01.06.2018.

[4] Crane. *PowerPoint, Microsoft Office 365 ProPlus*, version 16.0.9126.2210, Microsoft, 2016.

[5] Satellite Dish. *PowerPoint, Microsoft Office 365 ProPlus*, version 16.0.9126.2210, Microsoft, 2016.

[6] ITU-R, "Propagation data and prediction methods required for the design of terrestrial line-of-sight systems," Tech. Rep. P.530-17, International Telecommunication Union, Dec 2017.

[7] Photocopier. *PowerPoint, Microsoft Office 365 ProPlus*, version 16.0.9126.2210, Microsoft, 2016.

[8] Wireless Router. *PowerPoint, Microsoft Office 365 ProPlus*, version 16.0.9126.2210, Microsoft, 2016.

[9] Smart Phone. *PowerPoint, Microsoft Office 365 ProPlus*, version 16.0.9126.2210, Microsoft, 2016.

[10] Icon made by Freepik from www.flaticon.com. `https://www.flaticon.com/free-icon/ship-front-view_61949.Accessed:23.05.2018`.

[11] ITU-R, "The radio refractive index: its formula and refractivity data," Tech. Rep. P.453-13, International Telecommunication Union, Dec 2017.

[12] ITU-R, "Reference standard atmospheres," Tech. Rep. P.835-6, International Telecommunication Union, Dec 2017.

[13] P. Plait, "How far away is the horizon?," *Discover Magazine*, Jan 2009.

[14] ITU-R, "Specific attenuation model for rain for use in prediction methods," Tech. Rep. P.838-3, International Telecommunication Union, Mar 2005.

[15] ITU-R, "Attenuation by atmospheric gases," Tech. Rep. P.676-10, International Telecommunication Union, Sep 2013.

[16] R. Coudé, "Fresnel zones." `http://radiomobile.pe1mew.nl/?Calculations:Propagation_calculation:Fresnel_zones`. Taken from Radio Mobile - RF propagation simulation software. Accessed: 24.02.2018.

[17] T. Henderson, "18. radio propagation models." `https://www.isi.edu/nsnam/ns/doc/node216.html`, 2011. Taken from Information Sciences Instutute. Accessed: 12.01.2018.

[18] A. Brydon, "Summary of 3gpp standards releases for lte," *Unwired Insight*, Oct 2012.

[19] 3rd Generation Partnership Project, "Lte ue-category." `http://www.3gpp.org/more/1612-ue-category`, 2016. Taken from 3PGG. Accessed: 11.05.2018.

[20] S. Kumar, "Ooredoo first in the world to launch 5g network," *The Peninsula*, May 2018.

[21] 3rd Generation Partnership Project, "Charging architecture and principles (release 15)," *3GPP TS 32.240*, vol. 15.

[22] 3rd Generation Partnership Project, "Evolved universal terrestrial radio access (e-utra); physical layer procedures," *3GPP TS 36.213*, vol. V15.1.0, Mar 2018.

[23] MarineTraffic, "Elisabeth knutsen." `https://www.marinetraffic.com/en/ais/details/ships/shipid:193627/mmsi:235064647/imo:9131357/vessel:ELISABETH_KNUTSEN`. Taken from MarineTraffic. Accessed 24.04.2015.

[24] ITU-R, "Propagation by diffraction," Tech. Rep. P.526-14, International Telecommunication Union, Jan 2018.

[25] C. Y. D. Sim, *The propagation of VHF and UHF radio waves over sea paths.* PhD thesis, University of Leicester, 2002.

[26] G. Lenkurt, *Engineering considerations for microwave communications systems.* Lenkurt Electric Company, 1970.

[27] L. J. Ippolito, *Radiowave propagation in satellite communications.* Springer Science & Business Media, 2012.

[28] K. Feher, *Wireless digital communications: modulation & spread spectrum applications.* Prentice-Hall, Inc., 1995.

[29] J. W. Mark and W. Zhuang, *Wireless communications and networking.* Prentice Hall, 2002.

[30] ITU-R, "Propagation data and prediction models for the planning of indoor radio-communication systems and radio local area networks in the frequency range 900 mhz to 100 ghz," Tech. Rep. P.1238-9, International Telecommunication Union, Jun 1997.

[31] ITU-R, "Propagation data and prediction methods for the planning of short-range outdoor radiocommunication systems and radio local area networks in the frequency range 300 mhz to 100 ghz," Tech. Rep. P.1411-9, International Telecommunication Union, Jun 2017.

[32] Y. H. Lee, F. Dong, and Y. S. Meng, "Near sea-surface mobile radiowave propagation at 5 ghz: Measurements and modeling," *Radioengineering*, vol. 23, 2014.

[33] J. P. Linnartz, "Path loss." http://www.wirelesscommunication.nl/reference/chaptr03/pathloss.htm, 1995. Taken from Wirelesscommunication.nl. Accessed 13.01.2018.

[34] I. Poole, "Radio signal path loss." http://www.radio-electronics.com/info/propagation/path-loss/rf-signal-loss-tutorial.php, 2018. Taken from Radio-Electronics.com. Accessed 14.01.2018.

[35] I. Poole, "What is radio propagation: Rf propagation." https://www.electronics-notes.com/articles/antennas-propagation/propagation-overview/basics.php, 2018. Taken from Electronics notes. Accessed 06.01.2018.

[36] S. Sesia, I. Toufik, and M. Baker, *LTE - the UMTS long term evolution*. Wiley, 2 ed., 2011.

[37] M. Willis, "Reflections from surfaces and objects." http://www.mike-willis.com/Tutorial/PF8.htm, 2007. Taken from Mike-willis.com. Accessed 13.01.2018.

[38] M. Willis, "Fixed systems." http://www.mike-willis.com/Tutorial/PFL.pdf, 2006. Taken from mike-willis.com.

Appendix A

Matlab scripts

This section gives a short description of each file attached to this document. These are scripts used to create most of the figures found throughout the thesis.

atmosphericGasesAttenuation folder

Holds all m.-files related to the atmospheric gas attenuation. Main files are *attenuation_frequency.m* and *attenuation_waterVapour.m*, which finds the attenuation in dB/km based on frequency and water vapour density, respectively. Other .m-files within this folder are functions/methods used by both main files.

bitErrorPlots.m

Simulation of bit errors, or symbol errors, finding the SER based on the channel SNR.

diffractionAttenuation.m

Finds the diffraction attenuation for both channel on a system with space diversity, as a function of a knife-edge obstacle's height.

freeSpacePathLoss.m

Finds the FSPL for distances up to 60 km, for four carriers between 800 MHz and 12 GHz.

groundReflecModel.m

Finds the predicted attenuation for distances up to 60 km, using the two-ray ground reflection model.

LTEblockAllocation.m & LTEblockAllocationUL.m

Plots the RB usage as a function of SINR for downlink and uplink, respectively.

LTEcellCapacity.m & LTEcellCapacityUL.m

Plots the SINR, CQI, RSSI and throughput as a function of RSRP for downlink and up-link, respectively.

rainAttenuation.m

Finds the rain attenuation for different rain rates as a function of frequency. Also graphs the total attenuation during very heavy rain for a few different frequencies, for distances up to 50 km.

rayleighCriterion.m

Graphs the Rayleigh criterion for smoothness, based on surface roughness and grazing angle.

refractiveIndex.m

Graphs the refractive index as a function of height. Uses data based on the averages through the summer winter months separately.

seaReflection.m

Graphs the mean coefficient in dB for frequencies between 800 MHz and 12 GHz, for distances between 10 and 50 km, and 4 and 5 km separately.

signalConstellation.m

Shows the received signal constellation of a 64-QAM system with an AWGN channel.

tidalVariation.m

Find the mean coefficient of a system with fixed frequency and propagation distance, but with oscillating antenna heights, tidal variations.